Epitaxy of emerging materials and advanced heterostructures for microelectronics and quantum sciences

Yeonjoo Lee[1], Soo Ho Choi[2,3], Hyunseok Kim[2,3*], Jinkyoung Yoo[1,*]

[1]Center for Integrated Nanotechnologies, Los Alamos National Laboratory, Los Alamos, NM 87545, United States of America

[2]Department of Electrical and Computer Engineering, University of Illinois Urbana–Champaign, Urbana, IL 61801, United States of America

[3]Nick Holonyak, Jr. Micro and Nanotechnology Laboratory, University of Illinois Urbana–Champaign, Urbana, IL 61801, United States of America

Keywords: Epitaxy, Semiconductors, heavy fermion materials, low-dimensional materials, microelectronics, quantum materials

*Corresponding authors: jyoo@lanl.gov, hyunseok@illinois.edu

Abstract

Epitaxy, a process to prepare crystalline materials in nanostructures and thin films, is the core technology for preparing high-quality materials as a key enabler of next-generation microelectronics and quantum information system. Progress in epitaxy has been expanding the choice of materials and their heterostructures beyond the combinations limited by materials compatibility. However, the improvement of material quality, physical implementation of materials with unique properties, and integration of incommensurate materials in an architecture have been the challenging issues. Emerging materials, including two-dimensional materials and quantum

materials, have opened opportunities to study epitaxy mechanisms and realize various functional devices. Acceleration of discovery and progress in epitaxy research should be accomplished by ‘understanding of epitaxy under various circumstances at multiple length scales’ and ‘integration of experiments and models.’ In the perspective, a basic summary of the status of epitaxially grown materials, the challenges in epitaxy research, and integration of modeling epitaxy and ultimate control of the epitaxy process with advanced characterization techniques are discussed.

1. Introduction

High-quality materials are a key enabler pushing the boundaries of basic science and engineering, as manifested in the modern backbone of semiconductors-based transistors and low-dimensional carrier gas channels.[1, 2] Epitaxy, a process to form crystalline materials on crystalline substrates, has been the core technology for such materials development. In microelectronics, for example, homoepitaxy of silicon (Si) is the first step of front-end-of-line (FEOL) processes, and heteroepitaxy of silicon-germanium alloys on Si was successfully adopted in early 2000s. Since then, various homo- and heteroepitaxy techniques have been developed and optimized for pushing the limits of integrated circuit (IC) scaling further by shifting the paradigm from two-dimensional (2D) to three-dimensional (3D) transistors, such as Fin field-effect transistors (FETs) and gate-all-around FETs.[3] In quantum materials research, it is the key to implementing diverse degrees of freedom of charge, spin, orbital, and lattices in solid states. A physical implementation involves strong correlation and innately exotic electronic band structure. Unconventional superconductivity, heavy fermions, volume collapse transitions, Kondo insulator, hidden order, and quantum criticality are representative phenomena manifested in quantum materials.[4-6] Over decades, interest in thin films and heterostructures of quantum materials has been growing because those can immediately open new domains for quantum materials design, which is not available in bulk materials.[7, 8]

Despite remarkable breakthroughs in microelectronics during the past few decades, the surging need for computing power makes it more challenging than ever before for technological advancement to keep up with the demands of the market. As a radically new approach for next-generation microelectronics, monolithic 3D heterogeneous integration (3DHI) is proposed to allow integration of devices on top of each other.[9] In 3DHI, device layers are either directly grown on

or transferred onto device substrates, realizing vertical arrangement of multiple ultrathin device layers without wafers between them. 3DHI enables the interconnection of devices in each tier directly without the need for through-silicon-vias, which not only substantially increases the density of vertical interconnects and bandwidth but also greatly reduces the ohmic loss and RC delay. 3DHI technology is thus regarded as a promising pathway for high-performance computing and for enabling new schemes like process-in-memory architecture. Furthermore, the integration of photonic, optoelectronic, and sensory devices with electronics via novel epitaxy and 3DHI approaches can enable new form factors, which can substantially enhance the performance of those devices, and more importantly, can achieve versatile platforms such as complementary metal-oxide semiconductor (CMOS) with emerging technologies (X) (CMOS+X), multi-modal sensors, and edge computing for internet-of-things.[10]

It is important to note that the development of new materials and their integration are crucial for realizing 3DHI. Most importantly, crystalline thin films are one of the key building blocks that constitute device layers for 3DHI, yet the integration processes for crystalline materials are not fully established. Figures 1(a) and (b) show a representative scheme of 3DHI system (a) and the relevant materials issues (b). The crystalline materials to be integrated and the materials underlying are both vastly different from those used in FEOL processes, which necessitate novel approaches for the integration of crystalline thin films in 3DHI. To address these issues, various crystalline materials and their integration techniques are being developed for 3DHI and advanced microelectronics. A representative example is van der Waals (vdW) materials, such as transition metal dichalcogenides (TMDs).[11] These materials are regarded as a promising candidate for crystalline channels in future transistors, because they exhibit high mobility even when they are atomically thin, which is in stark contrast to Si-based channels with their mobility substantially

dropping at the thickness below a few nanometers.[12] VdW materials also work as a unique template to allow novel epitaxy mechanisms on them, which could enable the synthesis of unprecedented crystalline materials and their heterostructures. However, there remain challenges for these crystalline materials and processes to be adopted for real-world applications, such as the material quality, uniformity, process compatibility, and mechanical/thermal stability. Holistic co-design approaches combining theory, growth, fabrication, and characterization are necessary to advance the technology.

Quantum information systems (QISs) are attracting tremendous interest to open new applications, such as spintronics based on control of spin texture transport, quantum computing hardware enabled by unconventional superconductivity and control of quasiparticles, low power switches realized by quantum anomalous Hall effect, and size-independent interconnects as depicted in Figure 1(c). Figure 1(d) shows the materials issues to realize the QISs in Figure 1(c), explorable in thin films of quantum materials. In other words, the quantum materials community is seeing opportunities to accomplish progress and breakthroughs, such as the integer and fractional quantum Hall effect, obtained in semiconductor heterostructures.[1, 2] Nevertheless, studies of quantum materials have mainly been limited to bulk crystals. The category of quantum materials encompasses a broad range of materials, such as 2D TMDs, Rare-earth (RE)-pnictides, and semi-metallic compounds. Stoichiometry of quantum materials is usually complicated as 115-type (e.g., $CeCoIn_5$), 122-type (e.g., $AEAFe_4As_4$ (*AE*=Ca, Sr, Ba, Eu / *A*=Na, K, Rb)) and others.[5, 8, 13-17] The high-purity precursors and sources of REs and chalcogens are not readily available. Moreover, there are no suitable substrates for various quantum materials. While transition metal oxides are being used as the substrates, their quality is not comparable to that of Si and III–V wafers. The relatively poor substrates/source materials and unestablished growth conditions result

in significant impurity and defect scattering of charge/energy carriers in quantum materials. Progress in epitaxy of quantum material thin films is required to deliver the expected broad and in-depth impacts described at the beginning of this section.

In this perspective, we discuss recent breakthroughs in epitaxy techniques and integration processes for developing crystalline materials for microelectronics and QISs. Chapter 2 describes representative epitaxial and non-epitaxial mechanisms for synthesizing crystalline materials. Chapter 3 introduces recent breakthroughs demonstrating novel crystalline materials and their heterostructures, which are unique and can be applied to developing other impactful material systems. Chapter 4 discusses current challenges in materials development and share our perspective for future directions.

2. General categories of epitaxy and deposition

Epitaxy process is commonly described as a combination of precursor adsorption, adatom migration, nucleation, and propagation of the adsorbed constituent atoms. Several epitaxy mechanisms are classified along interactions between substrates and overgrown layers. The initial interactions can occur either at dangling bonds of substrates (conventional way) or through vdW gap in case of layered materials (unconventional way). In addition to these epitaxial growth mechanisms, it is important to note that crystalline materials can also be deposited by non-epitaxial approaches. Such non-epitaxial approaches, although less explored, have substantial impact on heterogeneous integration, because amorphous or polycrystalline substrates can be utilized for growing single-crystalline thin films. Therefore, epitaxial and non-epitaxial growth techniques complement each other and expand the 3DHI technology. Here is a summary of the epitaxy mechanisms and status of epitaxy techniques.

2.1. Conventional epitaxy: Dangling bonds-based

Conventional epitaxy mechanisms are based on formation of bonds between substrate and overgrown layer and subsequent procedures to relax strain along the interfacial region. Dangling bonds are preferential sites for formation of the bonds and nucleation of structural defects. Conventional epitaxy techniques have developed strain relaxation mechanisms along routes minimizing structural defect formation. The main drivers of conventional epitaxy techniques are III–V on Si and oxides on Si because of demands in scalable manufacturing of compound semiconductors and oxides-based devices. Several representative strategies of conventional epitaxy techniques are 'introducing buffer layer,' 'epitaxial lateral overgrowth (ELO),' 'aspect ratio trapping (ART),' and 'growing on miscut and/or patterned substrates' as summarized in Figure 2. Often, multiple strategies are utilized to obtain high-quality epitaxial layers.

A classic example of conventional epitaxy governed by material compatibility is GaAs growth on Si for optoelectronic IC applications. Although molecular beam epitaxy growths of GaAs on Si were demonstrated in the 1980s,[18-20] the mismatch of lattice constants (~4% between GaAs and Si) and thermal expansion coefficients hinder obtaining high-quality GaAs layers on Si. A typical threading dislocation density (TDD) in GaAs on Si was ~10^9/cm^2 with introducing a simple buffer layer. After decadal efforts of defect reduction via the strategies described in Figure 2, recently, a typical TDD in GaAs on Si is in the range of low-10^6/cm^2 and low-10^7/cm^2.[21-23] The current record-low TDD is <10^6/cm^2 (9.3×10^5/cm^2).[24]

2.2. Non-dangling bonds-based: Van der Waals epitaxy, QvdW, Remote epitaxy

While conventional epitaxy forms covalent or ionic bonds between substrates and epilayers, growing epilayers on layered materials, such as 2D materials, with weak vdW interactions and the absence of surface dangling bonds have been studied.[25] These methods are categorized into vdW epitaxy, Quasi-vdW (QvdW) epitaxy, and remote epitaxy, depending on the materials and epitaxy mechanism. VdW epitaxy, where a dangling-bond-free epilayer is grown on a similarly bond-free surface as shown in Figure 3(a), was reported with the growth of a 2D Se layer on a 2D Te layer.[26] Since the discoveries and rediscoveries of 2D materials, such as graphene and TMDs, vdW epitaxy has been extensively studied for various 2D materials and their heterostructures. VdW epitaxy forms a vdW gap between the epilayer and the substrate through dipole interactions rather than ionic or covalent bonding. In vdW epitaxy, nucleation on the surface of the layered substrate is suppressed, and nucleation at the edges or grain boundaries of the 2D materials is preferred.[27-30] VdW epitaxy has expanded beyond 2D heterostructures to include the epitaxial growth of one-dimensional (1D)/2D mixed-dimensional heterostructures and 1D vdW heterostructures.[31-34]

Extension of vdW epitaxy onto and of 3D materials with surface dangling bonds has led the development of QvdW epitaxy, as shown in Figure 3(b). 3D materials (i.e., AlN, GaN, GaAs, etc.) contain dangling bonds on their surfaces, allowing nucleation via chemical bonding at the step edges or defects of the 2D substrates. However, other regions formed through lateral growth are bound by vdW interactions. The QvdW epitaxial behavior was reported in the growth of GaN on epitaxial graphene(EG)/SiC substrate.[35] However, it was difficult to prove the origin of GaN lattice orientation, as the orientations of EG, SiC, and the GaN epilayers were identical. Liu *et al.* observed the epitaxial relationship between AlN epilayer and transferred tri-layer graphene sheets at different angles onto an AlN (0001) wafer.[36] Various III-V compound semiconductors have been successfully grown on graphene and hexagonal boron nitride (hBN) via QvdW epitaxy.[37-39]

While both vdW epitaxy and QvdW epitaxy involve the growth of the epilayer influenced by the lattice orientation of layered and 2D materials as substrates, remote epitaxy allows growth of epilayer following the orientation of the underlying substrate beneath a 2D material between the epilayer and the substrate, as shown in Figure 3(c). The remote epitaxy in GaAs epilayer/monolayer graphene/GaAs substrate was reported in 2017.[40] Through in-depth studies of the remote epitaxy mechanisms by multiple groups, the current understanding of the governing factors of remote epitaxy are the following:[41-43] (1) ionicity of substrate and epilayer, (2) thickness of the 2D layer, (3) polarity of 2D layer, and (4) charge transfer mediated through the 2D layer. As the ionicity of the substrate increases, the potential fluctuations of the substrate become more pronounced, making it more likely for these fluctuations to penetrate the 2D layer. Additionally, lower polarity and thinner 2D layers result in less effective potential screening. Consequently, while the 2D material screens potential fluctuations from the substrate, remote interactions with adatoms on the surface are still possible, allowing the epilayer to grow following the orientation of the substrate beneath the 2D layer.

2.3. Growth of crystalline 2D materials via non-epitaxial techniquesa

Unlike epitaxial growths, non-epitaxially grown materials do not exhibit crystallographic relationship with underlying substrates. Nevertheless, single-crystalline materials can still be formed via non-epitaxial techniques. Non-epitaxial technique expands available choice of substrates for single-crystal material deposition from crystalline substrates to amorphous and polycrystalline substrates. Non-epitaxial growth techniques can thus be an impactful approach for 3DHI.

The majority of 2D material thin film growth studies have been conducted on amorphous substrates due to difficulties of controlling the growth of 2D materials on crystalline substrates.[44-46] SiO_2/Si substrates are widely used in growth of 2D materials because they offer advantages in estimating the thickness of 2D materials due to their refractive index contrast.[47] Therefore, the growth of 2D materials has important sub-topics of the preparation of crystalline materials via non-epitaxial techniques. Since 2D materials lack surface dangling bonds, growth is favored in the in-plane direction once a nucleus forms. This tendency, general on amorphous substrates, has led the growth of triangular or hexagonal single-crystal TMD grains on the amorphous SiO_2 layer.[48] In non-epitaxial techniques, aligning grains in a single direction is challenging, prompting the proposal of various methods to enlarge single 2D grains. For graphene, strategies like oxidizing the surface of Cu foil to suppress nucleation or local feeding of methane precursors have enabled the growth of graphene grains up to 1 inch in size.[49, 50] In contrast, for TMDs, seeding promoters containing aromatic molecules or alkali metal ions has been reported to suppress precursor desorption, allowing larger grain growth.[51-53] Similar to graphene, limiting precursor supply has led to the successful growth of millimeter-sized TMD grains.[54] However, as the grain size increases, these methods require more atoms, consequently slowing down the growth rate and limiting the scalability.

Recrystallization is a thermal treatment at temperatures below the melting point of the material to guide unstable atoms into a more energetically favorable state. This method has recently been employed to prepare catalytic metal substrates to grow single crystalline 2D materials. Prolonged contact-free annealing process promote grain growth of energetically stable grain,[55] recrystallization of oxidized polycrystalline Cu foils,[56] recrystallization of polycrystalline Cu foils on a graphite susceptor,[57] all of which can produce single-crystal Cu foils. A simple melting-

solidification process was proposed as an alternative method to create single-crystal metals on polycrystalline metal foils. These single-crystal (111) and high-index Cu foils are now utilized as substrates for the epitaxial growth of coherently aligned graphene, hBN, and TMDs in a large area.[57] Recently, the recrystallization method was directly applied to grow crystalline 2D materials in wafer scale. In 2021, Xu *et al*. deposited a polycrystalline 1T′-$MoTe_2$ film on an amorphous SiO_2/Si wafer followed by the attachment of a single-crystal 2H-$MoTe_2$ crystal on top. After that, the entire surface was encapsulated with an Al_2O_3 layer, and they created a small hole through both the 2H-$MoTe_2$ crystal and the 1T′-$MoTe_2$ film. The recrystallization of 1T′-$MoTe_2$ was activated by thermal annealing under Te atmosphere. The recrystallization was guided by the orientation of the attached 2H-$MoTe_2$ crystal, as Te was introduced only through the hole, resulting in the successful growth of a wafer-scale single-crystal 2H-$MoTe_2$ film (Figure 4(a)).[58] In addition, Lee *et al.* demonstrated the growth of circular hBN grains on a liquid Au surface. The B and N atoms at the edges of these circular grains were self-collimated through Coulomb interactions, and the merging of these grains eventually led to the formation of a single-crystal monolayer hBN film (Figure 4(b)).[59]

3. Recent progress in epitaxy and deposition

Recently, the development of new epitaxy and deposition mechanisms, as well as the utilization of layered materials not only enabled the growth of new types of crystalline materials, but also brought new insights into materials engineering to form heterostructures made of incommensurate materials. Such expansion of the choice of materials and heterostructures represents great promise for future microelectronics and QISs. This chapter introduces recent

advancements in epitaxial and non-epitaxial growth processes, enabling the improvement of material quality, the synthesis of materials with unique properties, and the formation of heterostructures that are incommensurate.

3.1. Engineering crystallinity

3.1.1. Minimization of unintentional interfacial reaction

Reactions at the interfaces between a substrate and an epilayer form an interfacial layer. A prominent example showing the effects of interfacial reactions is epitaxy of oxides on Si. Oxide electronics fabricated on Si has attracted much attention due to scalable manufacturing of oxide devices utilizing the functionalities, such as ferroelectricity, piezoelectricity, magnetism, and multiferroics.[60] However, the reactivity of the Si surface is the obstacle to the epitaxial growth of functional oxides on Si substrates. A metal surface phase has been typically formed to saturate dangling bonds on Si surface and protect the surface from oxidation. For instance, the formation of Sr–Si bonds enables the growth of $SrTiO_3$ (STO) on Si (100).[61, 62] In contrast to the elimination of interfacial oxide, utilization of an interfacial layer for the epitaxy of oxides on Si has also been explored. For instance, the polarization of $BaTiO_3$ on Si can be controlled by the MgO buffer layer generating tensile strain by large lattice mismatch.[63] The single-crystalline EuO films were achieved by the optimal oxidation of Si (001).[64]

3.1.2. Composition engineering by strain management

Various strategies have been proposed to address challenges such as strain and high dislocation density arising from conventional epitaxy. In 2019, Pasayat *et al.* demonstrated that introducing porosity into the GaN layer beneath the InGaN epilayer reduced the mechanical

stiffness and subsequently, accomplished effective strain relaxation in the InGaN epilayer (Figure 5(a)).[65] Another notable approach involves remote epitaxy and QvdW epitaxy on 2D materials. When epilayers are grown on a dangling-bond-free 2D substrate, only weak vdW interactions occur between the epilayer and the 2D substrate.[66] The vdW interactions reduce strain issues typically associated with strong covalent or ionic bonds in conventional epitaxy and lowers dislocation density (Figure 5(b)). Additionally, epitaxial growth on 2D materials has been reported to result in a lower migration barrier, leading to relatively reduced nucleation density and consequently lower dislocation density (Figure 5(c)).[42] Various research groups have successfully replicated the growth of strain-relaxed, high-quality epilayers on 2D materials. This has enabled the demonstration of high-performance light-emitting devices (LEDs) with uniform wavelength and enhanced emission intensity. This strategy is not limited to III–V semiconductors. Jiang *et al.* reported that halide perovskite grown via remote epitaxy on 2D materials exhibited lower TDD than those grown through ionic epitaxy (Figure 5(d)).[67] As a result, they observed a threefold increase in photoluminescence intensity and a four-fold enhancement in carrier lifetime.

3.2. Synthesizing unconventional crystals

In epitaxy, both thermodynamic and kinetic mechanisms influence the formation of crystalline thin films. Thermodynamically, the stable phase of materials is determined by growth temperature and pressure given by a phase diagram. For instance, various polytypes of SiC can be formed by tuning the growth conditions (e.g., 4H-SiC and 6H-SiC) and then cooling them down to room temperature, resulting in a metastable phase, where 3C-SiC is the stable phase at room temperature.

However, kinetic factors, such as formation energy, diffusion, and adsorption/desorption, also play critical roles. Substrate is also important because surface free energy of the substrate and interfacial strain affect nucleation and growth of the grown layer. Changing the material or the orientation of the substrate for epitaxy can yield the formation of completely different crystallographic orientations of the grown layers.[68] The kinetic factor offers opportunities to control crystal structures by employing 'non-standard' epitaxy environment, which enables the formation of crystalline thin films that are not thermodynamically favored at room temperature or under growth environment but are promising for microelectronic and QISs.

A well-known example dating back to 1980s is the growth of cubic-phase boron nitride (cBN). Although cBN is a favored phase at very high pressures, necessitating high-pressure high-temperature methods for the growth, ion beam-assisted deposition has enabled the growth of single-crystal cBN at low pressures and moderate temperatures.[69, 70] Providing excess kinetic energy by ion beam allows overcoming the energy barrier and removing unwanted phases of BN. Because cBN exhibits ultrawide-bandgap properties and can be doped to both *n*-type and *p*-type, ion beam-assisted deposition provides opportunities for high-power electronics based on cBN.

Recently, novel approaches to substrate and interface engineering have been proposed to synthesize materials with unprecedented phases. Intercalation-based formation of crystalline layers is a promising path for synthesizing atomically thin forms of traditionally bulk materials and harnessing exotic properties for various device applications. When materials are formed by intercalation, both the top and bottom sides of intercalated materials are interfaced with the surroundings, which is in stark contrast to typical epitaxy environment where only the bottom side (i.e., substrates) formed interfaces with as-grown materials. This provides opportunities to promote layer-by-layer growth, instead of Volmer-Weber type growth, to passivate sites of high surface

energy. Figure 6(a) shows that atomically thin and buckled 2D GaN can be formed by intercalation at the interface of EG/SiC, termed migration-enhanced encapsulated growth.[71] Similarly, various metals, such as Ga, In, and Sn, can be intercalated to form atomically thin and half-vdW metals at the EG/SiC interface.[72] The intercalated layers exhibit an epitaxial relationship with the substrate. Modified electronic band structures and superconductivity were experimentally observed from these 2D materials. Interstitial intercalation of Mg atoms into bulk GaN can form Mg/GaN superlattices exhibiting monolayer Mg epitaxially aligned with and sandwiched between a few-layer-thick GaN, as shown in Figure 6(b).[73] Huge uniaxial strain induced by the superlattice formation greatly enhances hole transport and reduces contact resistance.

Synthesis of thermodynamically unfavored materials by interface engineering can also be achieved by employing unconventional substrates. GaN, with its stable form being a hexagonal (i.e., wurtzite) phase, for instance, can be grown into a cubic (i.e., zinc-blende) phase by substrate engineering. A straightforward approach is to employ cubic substrates, such as SiC or GaAs,[74, 75] but lattice mismatch induces high density of dislocations and even the evolution of hexagonal GaN. A unique approach to resolve the challenge is to conduct selective-area epitaxy on V-grooved Si (100), where cubic GaN evolves from the interface of hexagonal GaN nuclei in the V-groove, as shown in Figure 6(c).[76, 77] Cubic GaN is polarization-free and exhibits smaller bandgap than hexagonal GaN, and such unique properties make cubic GaN a promising material for optoelectronic devices with high quantum efficiency and longer operation wavelengths.[78] Lonsdaleite (hexagonal) Ge is another example of the growth of unconventional phases on 2D materials. Growth of Si and Ge on wurtzite GaP nanowire can induce the formation of the hexagonal phase of group–IV semiconductors with direct band gap via structure transfer.[79] The

structure transfer-induced hexagonal Ge growth was also observed on sulfur-deficient monolayer MoS_2, of which in-plane crystal structure is hexagonal, as shown in Figure 6(d).[80]

3.3. Forming advanced heterostructures

Functional units in devices are interfacing different materials to form heterostructures. In the context of emerging 3DHI technology in microelectronics, developing adequate integration processes is also paramount. Recent breakthroughs in deposition and integration techniques enabled the formation of novel heterostructures in which the materials are incommensurate. This includes, but not limited to, single-crystalline materials formed on polycrystalline or amorphous templates, heterostructuring incommensurate crystalline materials (i.e. interfacing cubic and hexagonal layers), and heterostructuring crystalline materials with incommensurate in-plane alignments (i.e. two hexagonal layers stacked with arbitrary rotation angles other than 0, 30, or 60°), with significantly increases the degree of freedom for heterogeneous integration.

Single-crystal materials can be deposited on amorphous or polycrystalline substrates by engineering the nucleation, as briefly discussed in the section 2.3 and depicted in Figure 7(a). A notable example is confined epitaxy for growing 2D materials on amorphous substrates by confining the growth area using trenches and maintaining a single domain within each trench area.[81] Single-domain TMDs can be grown as arrays in defined areas at a wafer scale by geometrically confining the growth area. Monolayer TMDs as well as bilayer heterostructures of MoS_2/WSe_2 are successfully formed on SiO_2 substrates. Kinetic control of nucleation even enables the TMD domains to be perfectly aligned with each other, resulting in crystallographically aligned

TMD arrays on amorphous substrates by engineering the shape of trenches.[82, 83] Single-crystal TMD-based complementary FET architecture is also achieved by utilizing the technique to monolithically stacking pMOS, gate stack, nMOS, and another gate stack, all at BEOL-compatible temperatures,[82] representing a meaningful breakthrough for future microelectronics based on monolithic 3DHI.

The approach to forming a crystalline layer by controlling the number of seeds in a grain can also be applied to bulk materials, not only to 2D materials. A liquid-phase epitaxy achieves the orientation-controlled formation of III–V islands on SiO_2, using group III elements patterned and capped by dielectric, followed by transforming the elements into III–V compounds by providing group V precursors.[84, 85] The capability to form lateral heterojunctions in this approach could be suitable for high-mobility electronics and photonics for both CMOS and non-CMOS platforms.

Epitaxial growth for integrating materials with incommensurate crystal phases or in-plane orientation is also explored. In remote epitaxy, the 2D materials, typically graphene, exhibit no epitaxial relationships with the crystalline materials grown atop, as the nucleation occurs by interaction with underlying substrates through 2D layers.[40, 86, 87] This allows the formation of thin films with arbitrary phases on hexagonal 2D materials. The recent development on amorphous 2D materials-based remote epitaxy also expands the choice of materials to form incommensurate 3D/2D/3D heterostructures.[88]

Nucleation by vdW interaction also enables the formation of incommensurate 3D/2D/3D heterostructures. In QvdW epitaxy, crystalline films are epitaxially aligned with underlying 2D materials, whereas the 2D materials and the substrate do not necessarily possess epitaxial relationship. This provides opportunities to integrate thin films on incommensurate substrates, as

well as to tune the in-plane arrangement between them by engineering 2D materials.[36, 89] A novel approach to form 2D/3D/2D heterostructures with exotic in-plane arrangements is demonstrated by recrystallization of bulk materials sandwiched between 2D materials.[90] When gold nanoparticles between MoS_2 layers are annealed, twisted epitaxy mechanisms evolve to recrystallize nanoparticles and orient the Au (111) to the angle not commensurate with either the top or bottom MoS_2 as shown in Figure 7(b). The unique Moiré structure with periodic strain alters the electronic and optical properties of 2D/3D/2D heterostructures.

2D materials-based layer transfer processes can expand 3DHI technology further when combined with emerging epitaxy techniques. Thin films, which are grown on 2D materials by remote epitaxy or QvdW epitaxy, can be exfoliated from the substrate by mechanical exfoliation with atomic precision, thanks to the weak atomic bonding at the interface. The exfoliated crystalline layers can be transferred and bonded onto foreign templates for wafer-free 3DHI. This has enabled various novel electronic platforms, such as transferrable high-electron mobility transistors,[91] vertically stacking of LEDs with thin films transistors[92] and on flexible substrates,[93] and flexible electronics and sensors.[94, 95] For TMD channel-based microelectronics, forming gate stacks and metal contacts are a big challenge, and layer transfer techniques can contribute to forming ideal metal contacts[96] and gate stacks as depicted in Figure 7(c).[97] In summary, incommensurate heterostructures, enabled by purely growth-based approaches or by combining novel growth and transfer techniques, can serve as technologies for advanced 3DHI.

4. Challenges and Perspectives

The crucial future epitaxy research goals are 'high-quality materials' and 'improved process control.' Accomplishments of the goals are enabled by 'understanding of epitaxy under various circumstances at multiple length scales' and 'integration of experiments and models.' The two knobs have been evolutionary topics in epitaxy research. However, progress in modeling, characterization, and epitaxy techniques has turned the evolutionary topics into revolutionary and broadly impactful ones. In this chapter, modeling epitaxy, ultimate control of the nascent stage of epitaxy process, and integration of growth and characterization techniques are discussed as the key challenges in epitaxy research.

4.1. Materials design: Multi-scale modeling

Understanding and designing epitaxy process is an innate multi-scale problem. Epitaxy is formally described by four categories extending atomic scale to mesoscale and macroscale:[98] Thermodynamics of phase transition and interface formation, fluid dynamics of mass transport, statistical mechanics of crystal growth processes, and quantum mechanics of bond formation. Studying the physics of epitaxy has devised several crucial concepts of nucleation and growth models. However, there have been noticeable discrepancies between theoretical prediction and experiments over decades. For instance, in the 1980s, experiments on heteroepitaxy of device-quality GaAs on Si (211) and (100) substrates were contrary to then-theoretical expectations.[99] Recent progress in non-dangling bonds-based epitaxy techniques, such as vdW, QvdW, and remote epitaxy, has brought novel questions to understanding of epitaxy. Epitaxial growth of and on 2D materials including vdW gap has been understood by trend to accomplish highest possible symmetry between a 2D material and a substrate through aligned nucleation and subsequent

propagation of the growth front along atomic steps.[100-102] The initial model of non-dangling bonds-based epitaxy is being challenged by a very narrow experimental window enabling epitaxy of non-centrosymmetric 2D materials due to experimental observations showing that the atomic steps do not guide epitaxial growth.[103] Additionally, a recent study of vdW epitaxy elucidated strong correlation between in-plane and out-of-plane growth of layered materials, which was not considered in the previous models.[104] The history of epitaxy research shows that modeling and experiments are not integrated into an established framework. In most cases epitaxy models have been utilized to explain experimental observations rather than to predict and design of epitaxial growth processes.

A key challenge of modeling epitaxy is coupling atomistic and continuum length scales. In epitaxy, capturing long-range stress fields in bulk (substrate and overgrown layer), interface (substrate/overgrown layer), and surface (overgrown layer) is important to understand strain relaxation resulting in structural defects formation and morphological evolution in the epitaxial process. However, the long-range stress fields, calculated by continuum model, are governed by the atomic structure of the interface between the substrate and the overgrown layer. Therefore, a multi-scale model of epitaxy should couple atomic scale and macroscale which are calculated by different methods. Moreover, nucleation and morphology of epitaxial layer evolves over time. The time-dependent behaviors make modeling epitaxy more complicated. A recent demand for heteroepitaxy model of 2D/2D growth pushes limits of the complexity. Experimental results show that growths of graphene on hBN and of TMD on SiO_2 or Al_2O_3 take several hours.[105, 106] The combination of extended growth, the low adsorption coefficient of precursor molecules of a 2D material, and the rapid surface diffusion of precursor molecules and adatoms overwhelms calculations based on conventional models.[107]

To tackle the challenge of multi-scale modeling, several approaches, such as molecular dynamics/kinetic Monte Carlo–finite element method coupling, and phase-field method, have been devised.[107, 108] Figure 8 shows the bridging approach across atomistic scale to macroscale. A critical issue of multi-scale modeling is the required computing resources. Compared to first-principles calculation (e.g., density-functional-theory) and continuum model for macroscale calculation, mesoscale calculation requires tremendous computing capacity. Overcoming the resource issues requires developing novel algorithms, building of libraries of possible models, and fast feedback from databases of experimental results.[109, 110] Database and library construction were deemed expensive and time-consuming. However, advances in machine learning for materials science have brought the task into accomplishable domain.

Since the beginning of the 21st century, the utilization of neural networks to construct materials growth models has been explored.[111] In recent years, the automated and statistical analyses of growth process parameters have adopted machine learning.[112, 113] Epitaxy is considered as a highly complicated process due to the complexity of growth mechanisms and the large number of conditions affecting the grown material's quality, although a few parameters are controlled by human input. Nevertheless, machine learning has been successfully utilized to optimize growth parameters of various materials.[113-115] However, the current methodology in epitaxy monitoring obtains limited information. Moreover, most epitaxy studies generate a small number of limited parameters (temperature, pressure, precursor flows) because the results of epitaxy studies are obtained from human-conducted experiments and non-automated data collection except in manufacturing plants. The loss of critical data for epitaxy studies has been unavoidable. In the machine learning field, the issue is called a 'small data' problem. Available data are unbalanced and small size. The 'small data machine learning' problem is being overcome

by the development of algorithms including imbalanced learning cases.[116] There are various algorithms for small data machine learning: Support vector machine,[117] Gaussian process regression,[118] random forest,[119] gradient boosting decision tree,[120] XGBoost,[121] and symbolic regression.[121] Moreover, active learning and transfer learning are under development for handling small data obtained from material synthesis.[122, 123]

4.2. Nucleation control

The deposition and integration techniques described in previous sections represent promising candidates for future microelectronics and quantum applications. These techniques are still in their infancy, however, and there are several critical challenges that need to be addressed in nucleation and growth of crystalline materials.

It is crucial to develop growth processes that can enable reliable, controllable, and scalable nucleation. This is especially critical for the material systems involving 2D materials. When growing 2D materials, controlling the thickness and crystallinity is crucial to ensure uniform and high-performance devices. This is yet a challenging task, because the nucleation and growth mechanisms on microelectronic platforms are usually not self-limited. Wafer-scale growth of TMD layers with uniform thicknesses and crystallinity is challenging because of the sensitivity of adsorption, desorption, lateral overgrowth, and additional nucleation to the growth environment. Utilizing step edges and locally modifying surface properties are proposed as solutions for controllable nucleation of TMDs on conventional substrates[124] and 2D materials,[125] respectively. Non-epitaxial confined growth mechanisms are also proposed as a universal approach on arbitrary substrates, with the capability for deterministic nucleation.[82, 83] These studies strongly suggest

that engineering the substrate, either locally or as a whole, is as important as optimizing the growth parameters. Also, although these techniques have huge potential for bringing 2D materials into the mainstream of microelectronics, many of these methods are currently not compatible with industrial processes in terms of the substrate materials,[124, 126-128] processing temperature,[129-131] and the precursors used for the processes.[51-53] Theoretical understanding of the nucleation mechanisms with realistic considerations is the key for overcoming the challenges, and the multi-scale modeling and in-fab monitoring discussed in this section can contribute to tackling the issues.

Next, when using 2D materials as growth templates, such as in the case of remote epitaxy and QvdW epitaxy, preserving the 2D materials are another challenge because a high-temperature and reactive epitaxy environment can damage underlying 2D materials.[132-134] This can complicate the growth by inducing more than one growth mechanisms during the growth[86, 135] and, more importantly, negatively affect the quality of crystalline films grown by remote or QvdW epitaxy as demonstrated in Figure 9(a). Once 2D materials are damaged, the exfoliation of thin films becomes unreliable due to the direct bonding formed between epilayers and substrates through damaged areas of the 2D materials.[40] Therefore, it is crucial to investigate the possible damage to 2D materials at the nucleation stage.

Another challenge for nucleation on 2D materials stems from the extremely low surface free energy. Because of chemical inertness, the wetting on 2D materials is much poorer than that of conventional substrates. This can lead to the formation of crystalline defects and rough surfaces of thin films, thus undermining the usefulness and functionality of the technique. Such challenges in remote epitaxy and QvdW epitaxy can be addressed by various approaches; first, 2D materials with various properties need to be investigated, considering the type of thin films to be grown, to secure compatibility between the growth process and the materials, as well as to achieve the desired

nucleation. Second, engineering the properties of 2D materials can promote various nucleation mechanisms to ensure the formation of high-quality materials.[36, 136] Third, instead of adopting the nucleation conditions that have been optimized for conventional substrates, the nucleation conditions concerning the unique surface properties of 2D materials require investigation as illustrated in Figure 9(b).[137]

For other deposition techniques introduced in this perspective, such as utilizing unique substrate textures or employing intercalation/recrystallization mechanisms, similar challenges need to be addressed, such as the quality and uniformity of synthesized materials, as well as the repeatability, scalability, and compatibility of processes. Especially ensuring the uniformity and scalability of crystalline materials is critical for microelectronics, and the importance of growth template preparation cannot be overstated. Once the template is prepared, subsequent nucleation requires investigation, taking into account not only the unique surface properties of the template but also its dynamic nature, as the properties of the template materials may change under nucleation environments. This underscores the importance of growth monitoring and characterization, which will be discussed in the subsequent section.

4.3.Monitoring epitaxy process

Most epitaxial growth studies rely on ex-situ characterizations to analyze the grown epilayers or intermediate states to identify the underlying mechanisms. However, despite these *ex situ* techniques, there remain many challenges in fully elucidating the properties of various materials and understanding epitaxial growth mechanisms. Most of all, the analysis methods and procedures must be standardized. Currently, multiple techniques, such as X-ray diffraction (XRD),

electron backscatter diffraction, and Raman spectroscopy, are widely employed to analyze the crystallinity of epilayers. However, the measurement equipment and conditions significantly affect results, making it difficult to compare data across studies. Additionally, some conclusions are drawn based on only one or two types of data, leading to misunderstanding. This issue is particularly pronounced in the analysis of nanomaterials and their heterostructures, which have seen significant attention recently. The analysis techniques used in different studies often vary, and even when similar results are obtained, disparate interpretations and expressions make it challenging to reach clear conclusions. Therefore, standardizing measurement conditions for materials and equipment or developing models to convert data into comparable formats when conditions are recorded, could lead to a robust database enabling quantitative comparisons. Furthermore, cross-verifying results through at least three types of analysis would help eliminate erroneous conclusions and greatly assist in building a reliable database.

Relying on *ex situ* analyses, which are conducted after the growth process is completed, limits the ability to elucidate the nucleation and growth mechanisms as well as to control the growth process in real time. Additionally, there is a risk of altering the sample during transportation or in additional steps for analysis. Since these methods do not capture the intermediate states over very short time scales, there are inherent limitations in accurately determining the growth mechanisms. As a result, many studies on growth processes are increasingly using in-situ monitoring techniques, with efforts focused on developing better methods to overcome these challenges.

Over the past several decades, the most widely used technique for real-time monitoring of epilayer growth has been reflection high-energy electron diffraction (RHEED). Because RHEED allows for real-time surface structure analysis, it can be recorded to track the overall growth

process.[138] However, it is limited in providing structural information in the vertical direction and is highly sensitive to surface roughness. In addition, optical measurement techniques such as laser reflectometry have also been employed to analyze the thickness of epilayer, but they face challenges in determining the orientation relationship between the epilayer and the substrate.[139] While RHEED and optical measurement methods are predominantly used to observe the growth from a macroscopic perspective, real-time observation of the nucleation and phase transformation process at the atomic scale has also been actively conducted using *in situ* TEM techniques.[140, 141] Although *in situ* TEM offers such advantages, it can be challenging to replicate the exact environment of the growth chamber, which may lead to discrepancies between the observed processes and actual growth conditions. Recently, techniques such as *in situ* AFM applied to solution-based growth, as well as the integration of optical microscopy, Raman spectroscopy, and XRD within chambers or custom mini-chambers, have been reported.[142-145] These advancements allow for real-time observation of the actual growth modes and kinetics. Thus, various *in situ* growth monitoring techniques have been proposed to date, and they can be employed depending on the specific purpose. Developing equipment designs to accommodate these monitoring capabilities without altering growth environment is a holy grail for exploring materials growth.

Another issue in in-situ monitoring is time delays caused by the computing time needed to interpret measured data and by sensor response times. To address this, developing machine learning models capable of analyzing the monitoring results in real time (or predictively) and providing feedback to the process are essential. Furthermore, in large-area growth methods, such as chemical vapor deposition (CVD) and metalorganic CVD, *in situ* monitoring is typically limited to small, specific areas. Therefore, the development of a real time technique is highly desired to monitor the growth process across the entire surface.

In situ monitoring of epitaxial process of emerging materials has also been limited to characterization of structures. However, *in situ* analysis of growth process is being performed to elucidate the species impinged onto growth front and mass transport of the species as well. Therefore, monitoring capabilities identifying chemical species, such as mass spectrometry, absorption spectroscopy, fluorescence spectroscopy, and anti-stokes Raman scattering, are being required to be integrated into in-situ monitoring suite. Additionally, mass transport velocities of the species into the growth chamber and reactor can be monitored by laser Doppler anemometry. Quantitative information of reactants and precursor fluxes can be data to establish a framework to elucidate the whole epitaxy process of emerging materials.

While various ex-situ and in-situ techniques are being used, many research groups tend to focus on their specific areas of expertise, leading to research biased toward one approach. Therefore, cross-validation of *in situ* and *ex situ* results, analyzed in different environments, is necessary to understand the materials' intrinsic properties and the growth mechanisms. Moreover, the development of an integrated hybrid system capable of applying current *ex situ* techniques in *in situ* environments would advance the material growth and process control from the nanoscale to the macroscale.

4.4. Structure-property-performance correlation: Materials Science's tetrahedron

Structure–Property–Processing–Performance relation, known as 'Materials Science Tetrahedron', is an essential guide to study materials and their processing. The majority of epitaxy studies show the 'Processing–Structure' relationship, represented by TEM and XRD results, or the 'Structure–(Device)Performance' relationship, represented by TEM and device characterization. However, structural characteristics cannot be one outstanding descriptor to evaluate the quality of

an epitaxial layer. For instance, a typical TDD of GaN heteroepitaxial thin film (10^9–10^{10}/cm^2) is several orders higher than that of GaAs thin film (10^7–10^8/cm^2). Nevertheless, the photoluminescence efficiency of GaN thin film is high enough to be utilized for commercialized light-emitting device applications because excited carriers and excitons in GaN are radiatively recombined prior to non-radiative recombination at defect sites due to the short exciton diffusion length in GaN (60–80 nm).[146] Reported carrier mobility–TDD relations also show non-linear trends and significant discrepancies between the experiments and theoretical calculations.[147-152] The dominant factor limiting carrier mobility depends on the material dimensions and the conditions of device operation and characterization. Different structural characteristics exhibit discorded trends as well. The study of epitaxial STO (001) film on Si (100) revealed that the full-width-at half-maximum of STO (002) rocking curve is insensitive to TDD.[153] The discrepancies described above indicate that crucial material parameters for evaluating the quality of epitaxially grown materials need to be specific to the materials of interest. For instance, epitaxy research of crystalline membranes prepared by vdW, QvdW, and remote epitaxy techniques for next-generation microelectronics should provide information on defect characteristics, such as doping concentration, defect states, and the properties at the interfaces between the 2D material as substrates and the overgrown layer. Although the electrical properties are imperative for designing devices, unconventional epitaxy research has mainly been focused on crystallinity. Developments in material and device characterization techniques over decades enable multi-modal characterization with high sensitivity and spatiotemporal resolution. Nevertheless, the characterization of emerging materials, including 2D materials with reasonably high throughput, is still challenging. For instance, applying deep level transient spectroscopy, a conventional and powerful technique providing quantitative information on defect levels and concentrations, is not

feasible for 2D materials and semi-metallic topological materials. To overcome the limitation, workflows integrating and orchestrating machine learning, multi-scale modeling, and multi-modal characterization are being developed.[154, 155]

5. Conclusion

Epitaxy will enable another leap in microelectronics and quantum materials research field, ardently waiting for high-quality, reproducible, and scalable materials. The modern epitaxy techniques have already led us to the realms of material combinations and quality, in which the conventional material compatibility issues of lattice mismatch and thermal expansion coefficients are overcome. However, discoveries of emerging materials and understandings of epitaxy mechanisms keep bringing demands on the developments of epitaxy techniques. Since most of the demands are for deliverables not available through conventional approaches, the demands should be fulfilled by integrating progresses in epitaxy techniques and models with assistances of learning and prediction algorithms, rather than developing individual components of epitaxy research.

Acknowledgment

This work was partly supported at CINT, a U.S. Department of Energy, office of Basic Energy Sciences User Facility at Los Alamos National Laboratory (Contract 89233218CNA000001) and Sandia National Laboratories (Contract DE-NA-0003525). Y. Lee and J. Yoo acknowledge support by the Laboratory Directed Research and Development program of Los Alamos National Laboratory (20230256ER). H. Kim acknowledges support by the National Science Foundation (ECCS-2328839) and the National Research Foundation of Korea (NRF) grant funded by the

Korea government (MSIT) (RS-2024-00445081 and RS-2024-00451173). S. H. Choi acknowledges support by the National Research Foundation of Korea funded by Ministry of Science and ICT (RS-2024-00339626).

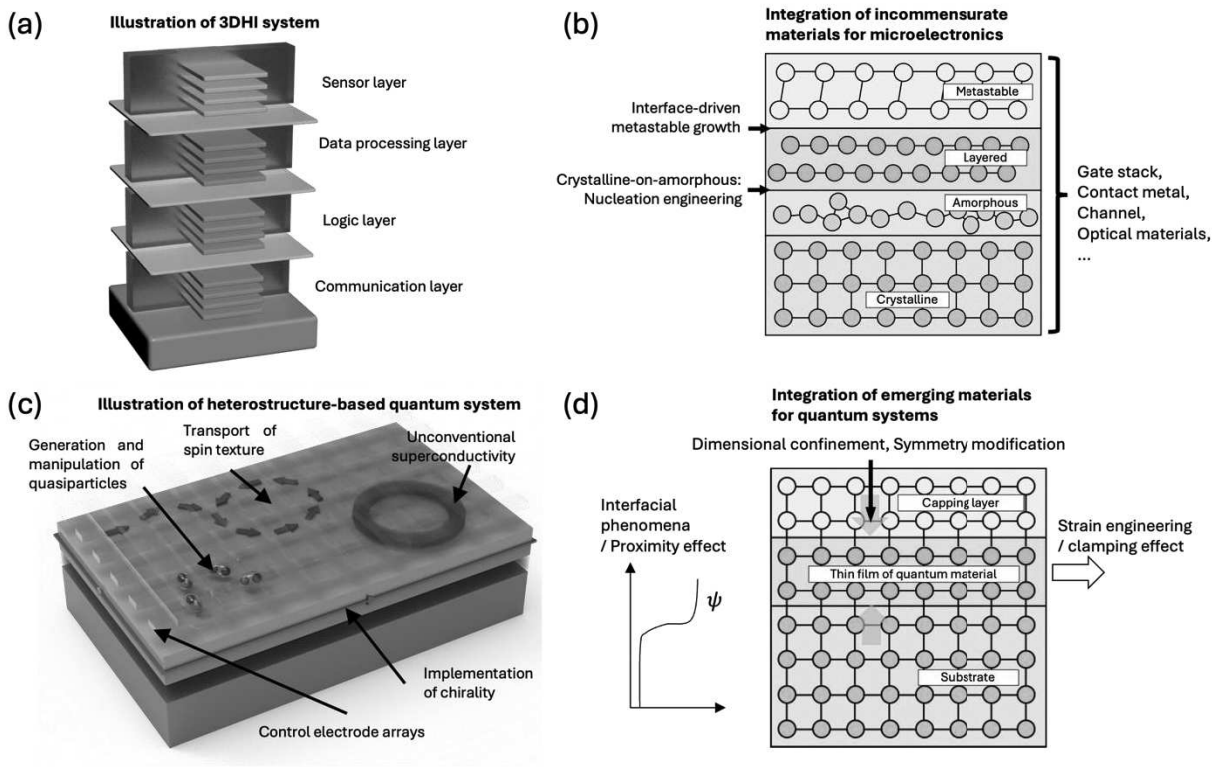

Figure 1. Scientific and technological opportunities enabled by epitaxy of microelectronics (a, b) and quantum materials (c, d).

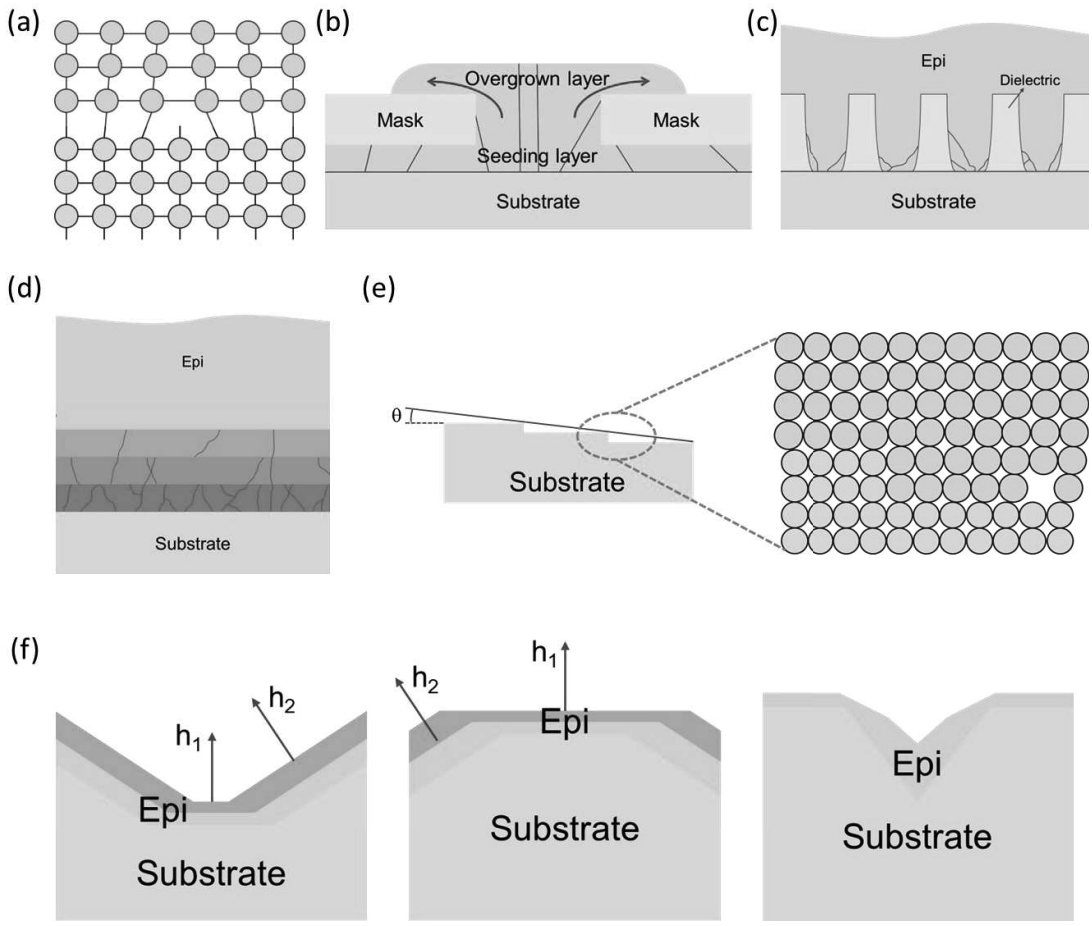

Figure 2. (a) The schematic of conventional epitaxy shows heteroepitaxy, which consists of the substrate and the epilayer in different materials. The dangling bond in the middle indicates misfit dislocation caused by lattice mismatch between two materials. (b) ELO improves the crystallographic quality of epitaxial layers by using a thin layer on a substrate as a starting point and introducing dielectric masks to prohibit the propagation of defects. The epitaxial layer continues to grow selectively in the mask's opening, where the seeding layer is exposed. The epitaxial layer starts to grow in the lateral direction above the height of the mask. The laterally grown layer is called ELO layer and exhibits lower defect density because dielectric masks can prohibit the defect propagation. (c) ART technique is a selective epitaxial growth to reduce defects by using a patterned substrate with vertical dielectric grooves with an aspect ratio greater than 2.

The defects are trapped at the bottom region of the grooves. (d) The buffer layer is introduced between a substrate and an epilayer to control and reduce the number of dislocation densities in the epilayer. It plays a role in relaxing stress caused by the mismatch of lattice constant or thermal expansion to improve the quality of epilayer. Structural defects such as TDs can be bent in a strain field in buffer layers and be prevented from penetrating into the epilayer. Two-step growth has been most widely used to heteroepitaxy; a buffer layer is grown at low temperature followed by high-temperature growth of an epilayer. (e) Miscut substrates have been employed to suppress the formation of APBs. For III–V layer growth on Si (001) bi-atomic steps on the Si surfaces suppress APBs. h_1 and h_2 indicate the growth rates on different crystal planes. (f) Patterned substrates are used to reduce TDD for heteroepitaxy. TDs can be confined in certain crystallographic planes when the epi-layer is grown on a patterned substrate.

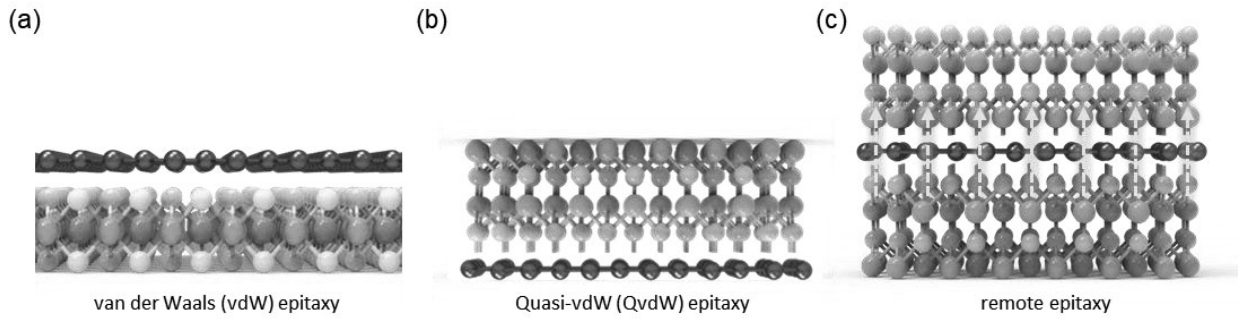

Figure 3. Non-dangling bonds-based epitaxy. Schematics of (a) vdW epitaxy, (b) QvdW epitaxy, and (c) remote epitaxy.

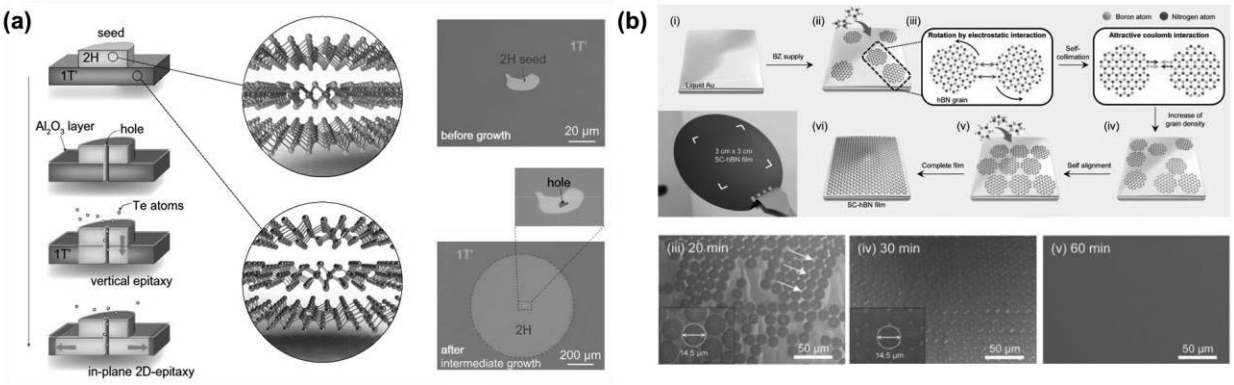

Figure 4. Novel approaches for the growth of single-crystalline 2D materials. (a) A schematic and optical images of recrystallizing polycrystalline 1T′-$MoTe_2$ into single-crystal 2H-$MoTe_2$ using a seed crystal. Te atoms are injected through a hole in the seed crystal, initiating recrystallization from the seed and allowing the growth of a single-crystal 2H-$MoTe_2$ film. Reproduced with permission.[58] Copyright 2021, The American Association for the Advancement of Science. (b) A schematic of the single-crystal hBN growth on a liquid Au surface, demonstrating how the circular hBN grains align to form a single-crystal hBN film, along with SEM images and photographs of the hBN grains and films. Circular hBN grains grown on liquid Au can move and rotate freely like icebergs on water, enabling alignment and coalescence into a single-crystal film. Reproduced with permission.[59] Copyright 2018, The American Association for the Advancement of Science.

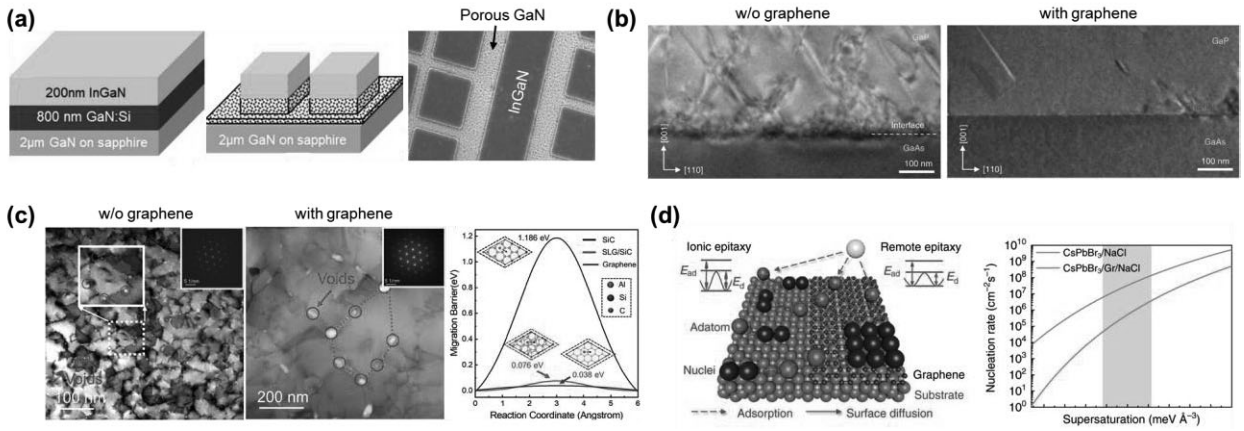

Figure 5. Strain engineering and quality improvement strategies. (a) A schematic and SEM image demonstrating strain relaxation using a porous structure. The strain in the InGaN layer is relaxed by making the underlying GaN layer porous. Reproduced with permission.[65] Copyright 2019, IOP Publishing Ltd. (b) Cross-sectional TEM images of GaP layer grown on bare GaAs and graphene-coated GaAs substrates. The GaP grown on the graphene-coated GaAs substrate shows significantly fewer dislocations. Reproduced with permission.[66] Copyright 2020, Springer Nature. (c) Plan-view BF-scanning transmission electron microscopy (STEM) images of AlN layers grown on SiC and single-layer graphene (SLG)/SiC substrates, along with the calculated migration barrier of Al atoms. Black, red, and blue lines represent the calculated migration barriers of Al atom on SiC, SLG/SiC, and graphene surfaces, respectively. The migration barrier on the dangling-bond-free graphene surface is lower, resulting in suppressed nucleation and the growth of a high-quality AlN layer. Reproduced with permission.[42] Copyright 2023, American Chemical Society. (d) A schematic of the nucleation process in ionic and remote epitaxy, and a plot showing the nucleation rates as a function of supersaturation for both ionic epitaxy ($CsPbBr_3$/NaCl) and remote epitaxy ($CsPbBr_3$/Gr/NaCl). Reproduced with permission.[67] Copyright 2019, Springer Nature.

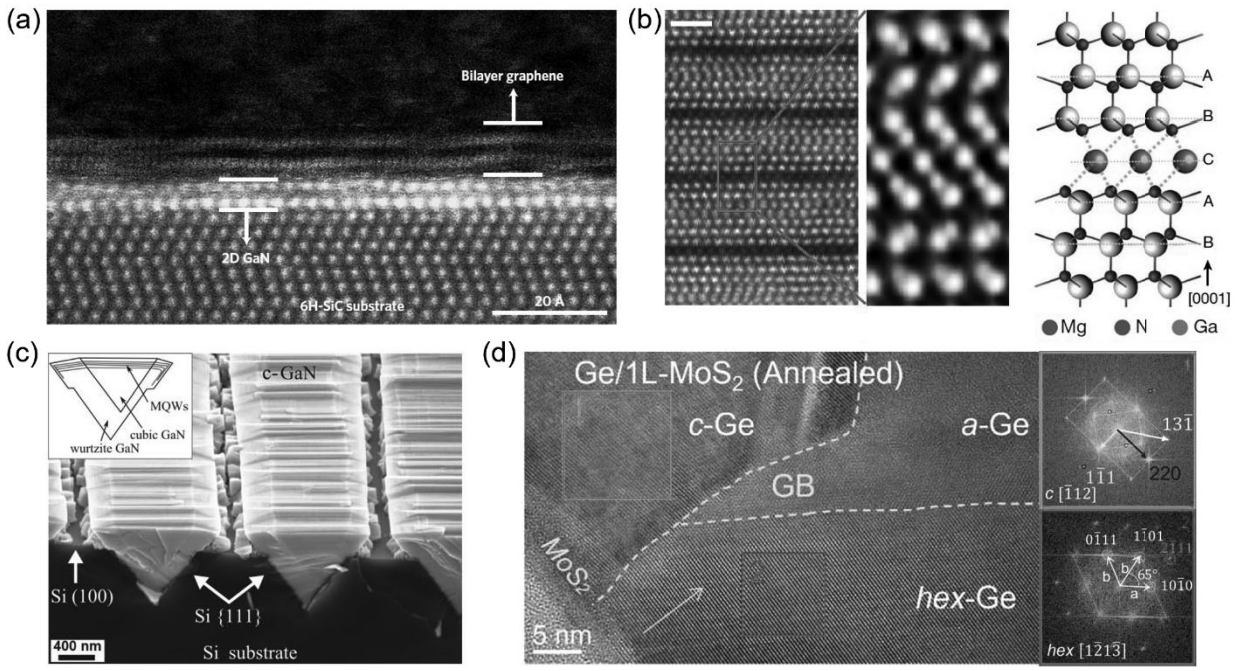

Figure 6. Realization of unconventional crystal structure. (a) Cross-sectional STEM image of 2D GaN formed at the interface between EG and SiC substrate by intercalation. Reproduced with permission.[71] Copyright 2016, Springer Nature. (b) Cross-sectional STEM image of 2D Mg-intercalated GaN superlattices. Reproduced with permission.[73] Copyright 2024, Springer Nature. (c) Cross-sectional SEM of c-GaN with quantum wells grown on a V-grooved Si (100). Reproduced with permission.[76] Copyright 2013, AIP Publishing. (d) Cross-sectional TEM image of a mixture of hexagonal and cubic Ge phases grown on sulfur-deficient monolayer MoS_2. Reproduced with permission.[80] Copyright 2023, Elsevier.

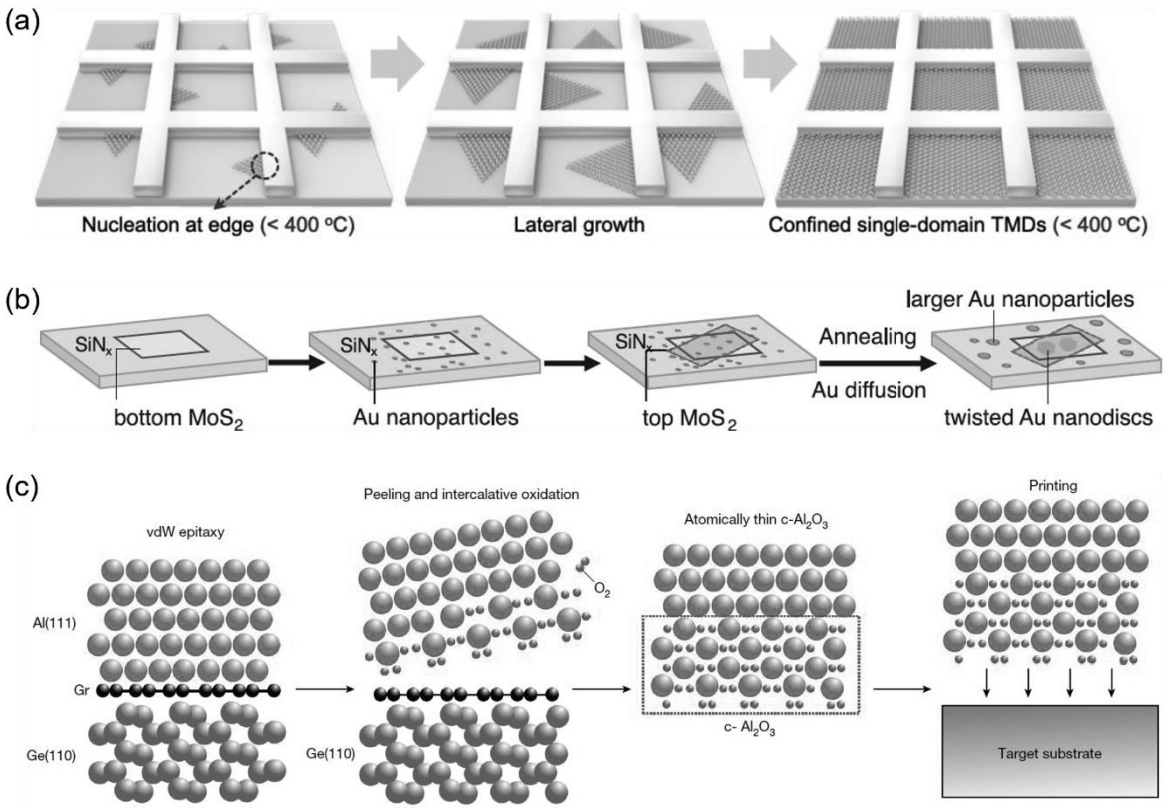

Figure 7. Novel heterostructure formation processes. (a) Process schematic of single-crystal TMD arrays growth on amorphous substrates with in-plane orientation control by pattern edges. Reproduced with permission.[82] Copyright 2023, arXiv. (b) Process schematic of crystalline Au nanodisc synthesis by twisted epitaxy. Reproduced with permission.[90] Copyright 2024, The American Association for the Advancement of Science. (c) Process schematic of forming crystalline Al_2O_3/Al gate stack by exfoliation from 2D materials followed by intercalative oxidation. Reproduced with permission.[97] Copyright 2024, Springer Nature.

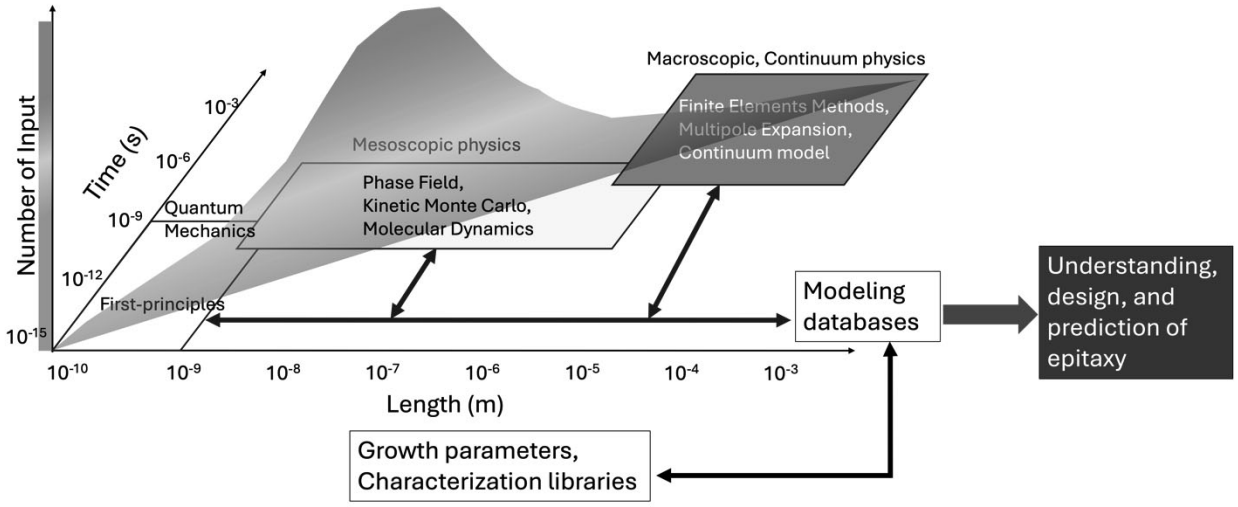

Figure 8. Domains and scheme of components of multi-scale modeling and the corresponding 'number of inputs.'

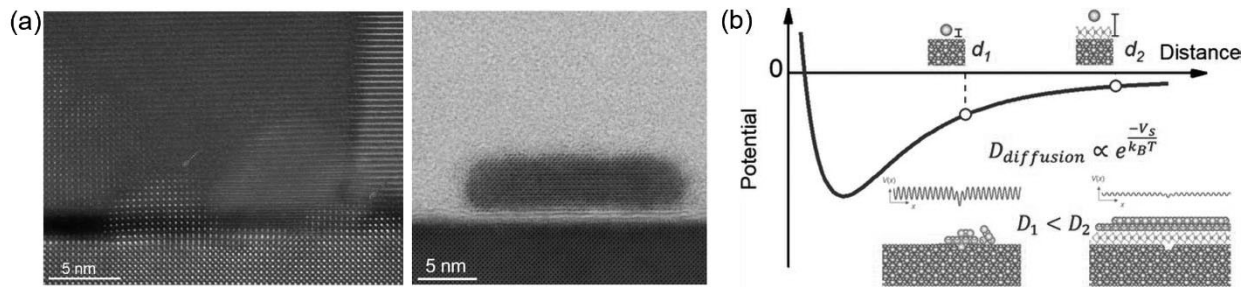

Figure 9. Controlling the nucleation. (a) STEM image showing direct growth through pinholes in damaged 2D materials (left). Remote epitaxial growth without pinholes, confirmed by imaging the entire island at nucleation stages (right). Reproduced with permission.[86] Copyright 2023, The American Association for the Advancement of Science. (b) Schematic illustrating lower potential barrier for adatom diffusion on 2D materials, enabling high-quality thin film growth at lower temperatures. Reproduced with permission.[137] Copyright 2022, American Chemical Society.

References

1. Klitzing, K. v.; Dorda, G.; Pepper, M., *Phys. Rev. Lett.* **1980,** *45* (6), 494.

2. Tsui, D. C.; Stormer, H. L.; Gossard, A. C., *Phys. Rev. Lett.* **1982,** *48* (22), 1559.

3. IEEE International Roadmap for Devices and Systems, "Beyond CMOS and Emerging Materials Integration". 2023.

4. Ronning, F.; Zhu, J.-X.; Das, T.; Graf, M.; Albers, R.; Rhee, H.; Pickett, W., *J. Phys. Condensed Matter* **2012,** *24* (29), 294206.

5. Herrera, E.; Guillamón, I.; Barrena, V.; Herrera, W. J.; Galvis, J. A.; Yeyati, A. L.; Rusz, J.; Oppeneer, P. M.; Knebel, G.; Brison, J. P., *Nature* **2023,** *616* (7957), 465-469.

6. Pfleiderer, C., *Rev. Mod. Phys.* **2009,** *81* (4), 1551-1624.

7. Chatterjee, S., *Electron. Struct.* **2021,** *3* (4), 043001.

8. Chatterjee, S.; Khalid, S.; Inbar, H. S.; Goswami, A.; Guo, T.; Chang, Y.-H.; Young, E.; Fedorov, A. V.; Read, D.; Janotti, A., *Sci. Adv.* **2021,** *7* (16), eabe8971.

9. IEEE International Roadmap for Devices and Systems - More Moore. 2023.

10. van Deurzen, L.; Kim, E.; Pieczulewski, N.; Zhang, Z.; Feduniewicz-Zmuda, A.; Chlipala, M.; Siekacz, M.; Muller, D.; Xing, H. G.; Jena, D.; Turski, H., *Nature* **2024,** *634* (8033), 334-340.

11. Radisavljevic, B.; Radenovic, A.; Brivio, J.; Giacometti, V.; Kis, A., *Nat. Nanotechnol.* **2011,** *6* (3), 147-150.

12. Uchida, K.; Watanabe, H.; Kinoshita, A.; Koga, J.; Numata, T.; Takagi, S. In *Experimental study on carrier transport mechanism in ultrathin-body SOI nand p-MOSFETs with SOI thickness less than 5 nm*, Digest. International Electron Devices Meeting, IEEE: **2002**; pp 47-50.

13. Izaki, M.; Shishido, H.; Kato, T.; Shibauchi, T.; Matsuda, Y.; Terashima, T., *Appl. Phys. Lett.* **2007,** *91* (12), 122507.

14. Kim, J.; Lee, H.; Lee, S.; Park, S.; Park, T.; Cho, Y.; Lee, H.; Kang, W. N.; Choi, W. S., *Curr. Appl. Phys.* **2019,** *19* (12), 1338-1342.

15. Inbar, H. S.; Ho, D. Q.; Chatterjee, S.; Pendharkar, M.; Engel, A. N.; Dong, J. T.; Khalid, S.; Chang, Y. H.; Guo, T.; Fedorov, A. V., *Phys. Rev. Mater.* **2022,** *6* (12), L121201.

16. Kölsch, S.; Schuck, A.; Huth, M.; Fedchenko, O.; Vasilyev, D.; Chernov, S.; Tkach, O.; Elmers, H.-J.; Schönhense, G.; Schlüter, C., *Phys. Rev. Mater.* **2022,** *6* (11), 115003.

17. Kawashima, K.; Ishida, S.; Fujihisa, H.; Gotoh, Y.; Yoshida, Y.; Eisaki, H.; Ogino, H.; Iyo, A., *Sci. Rep.* **2018,** *8* (1), 16827.

18. Wang, W., *Appl. Phys. Lett.* **1984,** *44* (12), 1149-1151.

19. Masselink, W.; Henderson, T.; Klem, J.; Fischer, R.; Pearah, P.; Morkoc, H.; Hafich, M.; Wang, P.; Robinson, G., *Appl. Phys. Lett.* **1984,** *45* (12), 1309-1311.

20. Uppal, P. N.; Kroemer, H., *J. Appl. Phys.* **1985,** *58* (6), 2195-2203.

21. Henriques, J.; Ilahi, B.; Heintz, A.; Morris, D.; Arès, R.; Boucherif, A., *J. Cryst. Growth* **2023,** *624*, 127433.

22. Yang, J.; Li, K.; Jia, H.; Deng, H.; Yu, X.; Jurczak, P.; Park, J.-S.; Pan, S.; Li, W.; Chen, S., *Nanoscale* **2022,** *14* (46), 17247-17253.

23. Jiang, C.; Liu, H.; Liu, Z.; Ye, J.; Zhai, H.; Liu, S.; Lin, J.; Wang, Q.; Ren, X., *Appl. Phys. A* **2024,** *130* (1), 5.

24. Shang, C.; Norman, J.; Gossard, A. C.; Bowers, J. E. In *GaAs Epitaxy on (001) Si: below 1×10^{6} cm^{-2} Dislocation Density with 2.4 μm Buffer Thickness*, 2020 Conference on Lasers and Electro-Optics (CLEO), IEEE: **2020**; pp 1-2.

25. Koma, A.; Ueno, K.; Saiki, K., *J. Cryst. Growth* **1991,** *111* (1), 1029-1032.

26. Koma, A.; Sunouchi, K.; Miyajima, T., *J. Vac. Sci. Technol. B* **1985,** *3* (2), 724-724.

27. Li, X.; Wu, G.; Zhang, L.; Huang, D.; Li, Y.; Zhang, R.; Li, M.; Zhu, L.; Guo, J.; Huang, T.; Shen, J.; Wei, X.; Yu, K. M.; Dong, J.; Altman, M. S.; Ruoff, R. S.; Duan, Y.; Yu, J.; Wang, Z.; Huang, X.; Ding, F.; Shi, H.; Tang, W., *Nat. Commun.* **2022,** *13* (1), 1773.

28. Zhou, X.; Liang, Y.; Fu, H.; Zhu, R.; Wang, J.; Cong, X.; Tan, C.; Zhang, C.; Zhang, Y.; Wang, Y.; Xu, Q.; Gao, P.; Peng, H., *Adv. Mater.* **2022,** *34* (42), 2202754.

29. Gao, W.; Dou, W.; Zhou, D.; Song, B.; Niu, T.; Hua, C.; Wee, A. T. S.; Zhou, M., *Small Methods* **2024,** *8* (10), 2301512.

30. Liu, L.; Ji, Y.; Bianchi, M.; Hus, S. M.; Li, Z.; Balog, R.; Miwa, J. A.; Hofmann, P.; Li, A.-P.; Zemlyanov, D. Y.; Li, Y.; Chen, Y. P., *Nat. Mater.* **2024,** *23* (10), 1339-1346.

31. Hong, Y. J.; Fukui, T., *ACS Nano* **2011,** *5* (9), 7576–7584.

32. Kim, Y.; Watt, J.; Ma, X.; Ahmed, T.; Kim, S.; Kang, K.; Luk, T. S.; Hong, Y. J.; Yoo, J., *ACS Nano* **2022,** *16* (2), 2399-2406.

33. Xiang, R.; Inoue, T.; Zheng, Y.; Kumamoto, A.; Qian, Y.; Sato, Y.; Liu, M.; Tang, D.; Gokhale, D.; Guo, J.; Hisama, K.; Yotsumoto, S.; Ogamoto, T.; Arai, H.; Kobayashi, Y.; Zhang, H.; Hou, B.; Anisimov, A.; Maruyama, M.; Miyata, Y.; Okada, S.; Chiashi, S.; Li, Y.; Kong, J.; Kauppinen, E. I.; Ikuhara, Y.; Suenaga, K.; Maruyama, S., *Science* **2020,** *367* (6477), 537-542.

34. Guo, J.; Xiang, R.; Cheng, T.; Maruyama, S.; Li, Y., *ACS Nanosci. Au* **2022,** *2* (1), 3-11.

35. Kim, J.; Bayram, C.; Park, H.; Cheng, C.-W.; Dimitrakopoulos, C.; Ott, J. A.; Reuter, K. B.; Bedell, S. W.; Sadana, D. K., *Nat. Commun.* **2014,** *5* (1), 4836.

36. Liu, F.; Wang, T.; Gao, X.; Yang, H.; Zhang, Z.; Guo, Y.; Yuan, Y.; Huang, Z.; Tang, J.; Sheng, B., *Sci. Adv.* **2023,** *9* (31), eadf8484.

37. Chen, Z.; Liu, Z.; Wei, T.; Yang, S.; Dou, Z.; Wang, Y.; Ci, H.; Chang, H.; Qi, Y.; Yan, J.; Wang, J.; Zhang, Y.; Gao, P.; Li, J.; Liu, Z., *Adv. Mater.* **2019,** *31* (23), 1807345.

38. Liang, D.; Wei, T.; Wang, J.; Li, J., *Nano Energy* **2020,** *69*, 104463.

39. Liu, F.; Wang, T.; Zhang, Z.; Shen, T.; Rong, X.; Sheng, B.; Yang, L.; Li, D.; Wei, J.; Sheng, S.; Li, X.; Chen, Z.; Tao, R.; Yuan, Y.; Yang, X.; Xu, F.; Zhang, J.; Liu, K.; Li, X.-Z.; Shen, B.; Wang, X., *Adv. Mater.* **2022,** *34* (5), 2106814.

40. Kim, Y.; Cruz, S. S.; Lee, K.; Alawode, B. O.; Choi, C.; Song, Y.; Johnson, J. M.; Heidelberger, C.; Kong, W.; Choi, S., *Nature* **2017,** *544* (7650), 340-343.

41. Kong, W.; Li, H.; Qiao, K.; Kim, Y.; Lee, K.; Nie, Y.; Lee, D.; Osadchy, T.; Molnar, R. J.; Gaskill, D. K., *Nat. Mater.* **2018,** *17* (11), 999-1004.

42. Wang, Y.; Qu, Y.; Xu, Y.; Li, D.; Lu, Z.; Li, J.; Su, X.; Wang, G.; Shi, L.; Zeng, X., *ACS Nano* **2023,** *17* (4), 4023-4033.

43. Wang, X.; Choi, J.; Yoo, J.; Hong, Y. J., *Nano Converg.* **2023,** *10* (1), 40.

44. Da, Y.; Zhou, Y.; Zhang, S.; Li, Y.; Jiang, T.; Zhu, W.; Chu, P. K.; Yu, X.-F.; Chen, X.; Wang, J., *Small* **2024,** *20* (30), 2310276.

45. Huangfu, Y.; Qin, B.; Lu, P.; Zhang, Q.; Li, W.; Liang, J.; Liang, Z.; Liu, J.; Liu, M.; Lin, X.; Li, X.; Saeed, M. Z.; Zhang, Z.; Li, J.; Li, B.; Duan, X., *Small* **2024,** *20* (28), 2309620.

46. Ma, Y.; Deng, Z.; Liang, H.; Guan, X.; Zheng, Z.; Yao, J.; Yang, G., *Laser & Photonics Rev.* **2024,** *18* (12), 2400669.

47. Ni, Z. H.; Wang, H. M.; Kasim, J.; Fan, H. M.; Yu, T.; Wu, Y. H.; Feng, Y. P.; Shen, Z. X., *Nano Lett.* **2007,** *7* (9), 2758-2763.

48. Wang, H.; Zhu, X.; Zhao, Z.; Wang, X.; Qian, Z.; Jiao, L.; Wang, K.; Li, Y.; Qi, J.-j.; Asif, M., *Nano Lett.* **2024,** *24* (18), 5498-5505.

49. Hao, Y.; Bharathi, M.; Wang, L.; Liu, Y.; Chen, H.; Nie, S.; Wang, X.; Chou, H.; Tan, C.; Fallahazad, B., *Science* **2013,** *342* (6159), 720-723.

50. Wu, T.; Zhang, X.; Yuan, Q.; Xue, J.; Lu, G.; Liu, Z.; Wang, H.; Wang, H.; Ding, F.; Yu, Q., *Nat. Mater.* **2016,** *15* (1), 43-47.

51. Ling, X.; Lee, Y.-H.; Lin, Y.; Fang, W.; Yu, L.; Dresselhaus, M. S.; Kong, J., *Nano Lett.* **2014,** *14* (2), 464-472.

52. Suleman, M.; Lee, S.; Kim, M.; Nguyen, V. H.; Riaz, M.; Nasir, N.; Kumar, S.; Park, H. M.; Jung, J.; Seo, Y., *ACS Omega* **2022,** *7* (34), 30074-30086.

53. Choi, S. H.; Kim, Y. J.; Yang, W.; Kim, K. K., *J. Kor. Phys. Soc.* **2019,** *74*, 1032-1038.

54. Gong, Y.; Ye, G.; Lei, S.; Shi, G.; He, Y.; Lin, J.; Zhang, X.; Vajtai, R.; Pantelides, S. T.; Zhou, W., *Adv. Funct. Mater.* **2016,** *26* (12), 2009-2015.

55. Jin, S.; Huang, M.; Kwon, Y.; Zhang, L.; Li, B.-W.; Oh, S.; Dong, J.; Luo, D.; Biswal, M.; Cunning, B. V., *Science* **2018,** *362* (6418), 1021-1025.

56. Li, Y.; Sun, L.; Chang, Z.; Liu, H.; Wang, Y.; Liang, Y.; Chen, B.; Ding, Q.; Zhao, Z.; Wang, R., *Adv. Mater.* **2020,** *32* (29), 2002034.

57. Wu, M.; Zhang, Z.; Xu, X.; Zhang, Z.; Duan, Y.; Dong, J.; Qiao, R.; You, S.; Wang, L.; Qi, J., *Nature* **2020,** *581* (7809), 406-410.

58. Xu, X.; Pan, Y.; Liu, S.; Han, B.; Gu, P.; Li, S.; Xu, W.; Peng, Y.; Han, Z.; Chen, J., *Science* **2021,** *372* (6538), 195-200.

59. Lee, J. S.; Choi, S. H.; Yun, S. J.; Kim, Y. I.; Boandoh, S.; Park, J.-H.; Shin, B. G.; Ko, H.; Lee, S. H.; Kim, Y.-M., *Science* **2018,** *362* (6416), 817-821.

60. Kumah, D. P.; Ngai, J. H.; Kornblum, L., *Adv. Funct. Mater.* **2020,** *30* (18), 1901597.

61. Tatsuyama, T. T., *Jpn. J. Appl. Phys.* **1998,** *37* (8R), 4454.

62. Spreitzer, M.; Klement, D.; Parkelj Potočnik, T.; Trstenjak, U.; Jovanović, Z.; Nguyen, M. D.; Yuan, H.; Ten Elshof, J. E.; Houwman, E.; Koster, G., *APL Mater.* **2021,** *9* (4), 040701.

63. Reynaud, M.; Huyan, H.; Du, C.; Li, W.; Posadas, A. B.; Pan, X.; Demkov, A. A., *ACS Appl. Electron. Mater.* **2023,** *5* (8), 4605-4614.

64. Averyanov, D. V.; Sokolov, I. S.; Taldenkov, A. N.; Kondratev, O. A.; Parfenov, O. E.; Tokmachev, A. M.; Storchak, V. G., *J. Mater. Chem. C* **2023,** *11* (16), 5481-5489.

65. Pasayat, S. S.; Gupta, C.; Acker-James, D.; Cohen, D. A.; DenBaars, S. P.; Nakamura, S.; Keller, S.; Mishra, U. K., *Semicond. Sci. Technol.* **2019,** *34* (11), 115020.

66. Bae, S.-H.; Lu, K.; Han, Y.; Kim, S.; Qiao, K.; Choi, C.; Nie, Y.; Kim, H.; Kum, H. S.; Chen, P., *Nat. Nanotechnol.* **2020,** *15* (4), 272-276.

67. Jiang, J.; Sun, X.; Chen, X.; Wang, B.; Chen, Z.; Hu, Y.; Guo, Y.; Zhang, L.; Ma, Y.; Gao, L., *Nat. Commun.* **2019,** *10* (1), 4145.

68. Nair, S.; Yang, Z.; Lee, D.; Guo, S.; Sadowski, J. T.; Johnson, S.; Saboor, A.; Li, Y.; Zhou, H.; Comes, R. B., *Nat. Nanotechnol.* **2023,** *18* (9), 1005-1011.

69. Inagawa, K.; Watanabe, K.; Saitoh, K.; Yuchi, Y.; Itoh, A., *Surf. Coat. Technol.* **1989,** *39*, 253-264.

70. Zhang, X.; Boyen, H.-G.; Deyneka, N.; Ziemann, P.; Banhart, F.; Schreck, M., *Nat. Mater.* **2003,** *2* (5), 312-315.

71. Al Balushi, Z. Y.; Wang, K.; Ghosh, R. K.; Vilá, R. A.; Eichfeld, S. M.; Caldwell, J. D.; Qin, X.; Lin, Y.-C.; DeSario, P. A.; Stone, G., *Nat. Mater.* **2016,** *15* (11), 1166-1171.

72. Briggs, N.; Bersch, B.; Wang, Y.; Jiang, J.; Koch, R. J.; Nayir, N.; Wang, K.; Kolmer, M.; Ko, W.; De La Fuente Duran, A., *Nat. Mater.* **2020,** *19* (6), 637-643.

73. Wang, J.; Cai, W.; Lu, W.; Lu, S.; Kano, E.; Agulto, V. C.; Sarkar, B.; Watanabe, H.; Ikarashi, N.; Iwamoto, T., *Nature* **2024,** *631*, 67-72.

74. Wei, C.; Xie, Z.; Li, L.; Yu, Q.; Edgar, J., *J. Electron. Mater.* **2000,** *29*, 317-321.

75. Nakadaira, A.; Tanaka, H., *J. Electron. Mater.* **1997,** *26*, 320-324.

76. Stark, C. J.; Detchprohm, T.; Lee, S.; Jiang, Y.-B.; Brueck, S.; Wetzel, C., *Appl. Phys. Lett.* **2013,** *103* (23), 232107.

77. Bayram, C.; Ott, J. A.; Shiu, K. T.; Cheng, C. W.; Zhu, Y.; Kim, J.; Razeghi, M.; Sadana, D. K., *Adv. Funct. Mater.* **2014,** *24* (28), 4492-4496.

78. Leszczynski, M.; Teisseyre, H.; Suski, T.; Grzegory, I.; Bockowski, M.; Jun, J.; Porowski, S.; Pakula, K.; Baranowski, J.; Foxon, C., *Appl. Phys. Lett.* **1996,** *69* (1), 73-75.

79. Hauge, H. I. T.; Verheijen, M. A.; Conesa-Boj, S.; Etzelstorfer, T.; Watzinger, M.; Kriegner, D.; Zardo, I.; Fasolato, C.; Capitani, F.; Postorino, P.; Kölling, S.; Li, A.; Assali, S.; Stangl, J.; Bakkers, E. P. A. M., *Nano Lett.* **2015,** *15* (9), 5855-5860.

80. Wang, X.; Kaufmann, R.; Jones, A. C.; Chen, R.; Ahmed, T.; Pettes, M. T.; Kotula, P. G.; Bilgin, I.; Wang, Y.; Kar, S., *Mater. Today Adv.* **2023,** *19*, 100401.

81. Kim, K. S.; Lee, D.; Chang, C. S.; Seo, S.; Hu, Y.; Cha, S.; Kim, H.; Shin, J.; Lee, J.-H.; Lee, S., *Nature* **2023,** *614* (7946), 88-94.

82. Kim, K. S.; Seo, S.; Kwon, J.; Lee, D.; Kim, C.; Ryu, J.-E.; Kim, J.; Song, M.-K.; Suh, J. M.; Jung, H.-G., *arXiv preprint arXiv:2312.03206* **2023**.

83. Groven, B.; Kandybka, I.; Voronenkov, V.; Vranckx, D.; Medina, H.; Nijs, S.; Kumar, P.; Moussa, A.; Saib, M.; Beggiato, M., **2024**. DOI 10.21203/rs.3.rs-4504047/v1.

84. Sarkar, D.; Wang, W.; Mecklenburg, M.; Clough, A. J.; Yeung, M.; Ren, C.; Lin, Q.; Blankemeier, L.; Niu, S.; Zhao, H., *ACS Nano* **2018,** *12* (6), 5158-5167.

85. Sarkar, D.; Tao, J.; Ahsan, R.; Yang, D.; Orvis, T.; Weng, S.; Greer, F.; Ravichandran, J.; Sideris, C.; Kapadia, R., *ACS Appl. Electron. Mater.* **2020,** *2* (7), 1997-2002.

86. Chang, C. S.; Kim, K. S.; Park, B.-I.; Choi, J.; Kim, H.; Jeong, J.; Barone, M.; Parker, N.; Lee, S.; Zhang, X., *Sci. Adv.* **2023,** *9* (42), eadj5379.

87. Chen, Q.; Yang, K.; Shi, B.; Yi, X.; Wang, J.; Li, J.; Liu, Z., *Adv. Mater.* **2023,** *35* (18), 2211075.

88. Kim, H.; Liu, Y.; Lu, K.; Chang, C. S.; Sung, D.; Akl, M.; Qiao, K.; Kim, K. S.; Park, B.-I.; Zhu, M., *Nat. Nanotechnol.* **2023,** *18* (5), 464-470.

89. Yin, Y.; Liu, B.; Chen, Q.; Chen, Z.; Ren, F.; Zhang, S.; Liu, Z.; Wang, R.; Liang, M.; Yan, J., *Small* **2022,** *18* (41), 2202529.

90. Cui, Y.; Wang, J.; Li, Y.; Wu, Y.; Been, E.; Zhang, Z.; Zhou, J.; Zhang, W.; Hwang, H. Y.; Sinclair, R., *Science* **2024,** *383* (6679), 212-219.

91. Glavin, N. R.; Chabak, K. D.; Heller, E. R.; Moore, E. A.; Prusnick, T. A.; Maruyama, B.; Walker Jr, D. E.; Dorsey, D. L.; Paduano, Q.; Snure, M., *Adv. Mater.* **2017,** *29* (47), 1701838.

92. Shin, J.; Kim, H.; Sundaram, S.; Jeong, J.; Park, B.-I.; Chang, C. S.; Choi, J.; Kim, T.; Saravanapavanantham, M.; Lu, K., *Nature* **2023,** *614* (7946), 81-87.

93. Jeong, J.; Wang, Q.; Cha, J.; Jin, D. K.; Shin, D. H.; Kwon, S.; Kang, B. K.; Jang, J. H.; Yang, W. S.; Choi, Y. S., *Sci. Adv.* **2020,** *6* (23), eaaz5180.

94. Kim, Y.; Suh, J. M.; Shin, J.; Liu, Y.; Yeon, H.; Qiao, K.; Kum, H. S.; Kim, C.; Lee, H. E.; Choi, C., *Science* **2022,** *377* (6608), 859-864.

95. Wang, D.; Lu, Y.; Meng, J.; Zhang, X.; Yin, Z.; Gao, M.; Wang, Y.; Cheng, L.; You, J.; Zhang, J., *Nanoscale* **2019,** *11* (19), 9310-9318.

96. Liu, Y.; Guo, J.; Zhu, E.; Liao, L.; Lee, S.-J.; Ding, M.; Shakir, I.; Gambin, V.; Huang, Y.; Duan, X., *Nature* **2018,** *557* (7707), 696-700.

97. Zeng, D.; Zhang, Z.; Xue, Z.; Zhang, M.; Chu, P. K.; Mei, Y.; Tian, Z.; Di, Z., *Nature* **2024**, 1-7.

98. Herman, M. A.; Richter, W.; Sitter, H., *Epitaxy: physical principles and technical implementation*. Springer Science & Business Media: **2013**; Vol. 62.

99. Kroemer, H., *J. Cryst. Growth* **1987,** *81* (1-4), 193-204.

100. Arciprete, F.; Boschker, J. E.; Cecchi, S.; Zallo, E.; Bragaglia, V.; Calarco, R., *Adv. Mater. Interfaces* **2022,** *9* (9), 2101556.

101. Dong, J.; Zhang, L.; Dai, X.; Ding, F., *Nat. Commun.* **2020,** *11* (1), 5862.

102. Reidy, K.; Thomsen, J. D.; Lee, H. Y.; Zarubin, V.; Yu, Y.; Wang, B.; Pham, T.; Periwal, P.; Ross, F. M., *Nano Lett.* **2022,** *22* (14), 5849-5858.

103. Zheng, P.; Wei, W.; Liang, Z.; Qin, B.; Tian, J.; Wang, J.; Qiao, R.; Ren, Y.; Chen, J.; Huang, C., *Nat. Commun.* **2023,** *14* (1), 1-7.

104. Hu, L.; Liu, D.; Zheng, F.; Yang, X.; Yao, Y.; Shen, B.; Huang, B., *Phys. Rev. Lett.* **2024,** *133* (4), 046102.

105. Zhou, H.; Yu, W. J.; Liu, L.; Cheng, R.; Chen, Y.; Huang, X.; Liu, Y.; Wang, Y.; Huang, Y.; Duan, X., *Nat. Commun.* **2013,** *4* (1), 2096.

106. Kang, K.; Xie, S.; Huang, L.; Han, Y.; Huang, P. Y.; Mak, K. F.; Kim, C.-J.; Muller, D.; Park, J., *Nature* **2015,** *520* (7549), 656-660.

107. Posthuma de Boer, J.; Ford, I. J.; Kantorovich, L.; Vvedensky, D. D., *J. Chem. Phys.* **2018,** *149* (19), 194107.

108. Lidorikis, E.; Bachlechner, M. E.; Kalia, R. K.; Nakano, A.; Vashishta, P., *Phys. Rev. B* **2005,** *72* (11), 115338.

109. Van Der Giessen, E.; Schultz, P. A.; Bertin, N.; Bulatov, V. V.; Cai, W.; Csányi, G.; Foiles, S. M.; Geers, M. G.; González, C.; Hütter, M., *Model. Simul. Mater. Sci. Eng.* **2020,** *28* (4), 043001.

110. Capone, M.; Romanelli, M.; Castaldo, D.; Parolin, G.; Bello, A.; Gil, G.; Vanzan, M., *ACS Phys. Chem. Au* **2024,** *4* (3), 202-225.

111. Lee, K. K.; Brown, T.; Dagnall, G.; Bicknell-Tassius, R.; Brown, A.; May, G. S., *IEEE Transac. Semicond. Manuf.* **2000,** *13* (1), 34-45.

112. Harris, S. B.; Rouleau, C. M.; Xiao, K.; Vasudevan, R. K., *npj Comput. Mater.* **2024,** *10* (1), 105.

113. Shen, C.; Zhan, W.; Xin, K.; Li, M.; Sun, Z.; Cong, H.; Xu, C.; Tang, J.; Wu, Z.; Xu, B., *Nat. Commun.* **2024,** *15* (1), 2724.

114. Wakabayashi, Y. K.; Otsuka, T.; Krockenberger, Y.; Sawada, H.; Taniyasu, Y.; Yamamoto, H., *APL Mater.* **2019,** *7* (10), 101114.

115. Ohkubo, I.; Hou, Z.; Lee, J. N.; Aizawa, T.; Lippmaa, M.; Chikyow, T.; Tsuda, K.; Mori, T., *Mater. Today Phys.* **2021,** *16*, 100296.

116. Xu, P.; Ji, X.; Li, M.; Lu, W., *npj Comput. Mater.* **2023,** *9* (1), 42.

117. Smola, A. J.; Schölkopf, B., *Stat. Comput.* **2004,** *14*, 199-222.

118. Deringer, V. L.; Bartók, A. P.; Bernstein, N.; Wilkins, D. M.; Ceriotti, M.; Csányi, G., *Chem. Rev.* **2021,** *121* (16), 10073-10141.

119. Talekar, B.; Agrawal, S., *Biosci. Biotechnol. Res. Commun* **2020,** *13* (14), 245-248.

120. Biau, G.; Cadre, B.; Rouvière, L., *Mach. Learn.* **2019,** *108*, 971-992.

121. Duan, J.; Asteris, P. G.; Nguyen, H.; Bui, X.-N.; Moayedi, H., *Eng. Comput.* **2021,** *37*, 3329-3346.

122. Lookman, T.; Balachandran, P. V.; Xue, D.; Yuan, R., *npj Comput. Mater.* **2019,** *5* (1), 21.

123. Ranaweera, M.; Mahmoud, Q. H., *Electronics* **2021,** *10* (12), 1491.

124. Li, T.; Guo, W.; Ma, L.; Li, W.; Yu, Z.; Han, Z.; Gao, S.; Liu, L.; Fan, D.; Wang, Z., *Nat. Nanotechnol.* **2021,** *16* (11), 1201-1207.

125. Li, J.; Yang, X.; Liu, Y.; Huang, B.; Wu, R.; Zhang, Z.; Zhao, B.; Ma, H.; Dang, W.; Wei, Z., *Nature* **2020,** *579* (7799), 368-374.

126. Chen, L.; Liu, B.; Ge, M.; Ma, Y.; Abbas, A. N.; Zhou, C., *ACS Nano* **2015,** *9* (8), 8368-8375.

127. Dumcenco, D.; Ovchinnikov, D.; Marinov, K.; Lazic, P.; Gibertini, M.; Marzari, N.; Sanchez, O. L.; Kung, Y.-C.; Krasnozhon, D.; Chen, M.-W., *ACS Nano* **2015,** *9* (4), 4611-4620.

128. Krishna, S.; Choi, S. H.; Kim, S. M.; Kim, K. K., *Curr. Appl. Phys.* **2024,** *59*, 208-213.

129. Boandoh, S.; Choi, S. H.; Park, J. H.; Park, S. Y.; Bang, S.; Jeong, M. S.; Lee, J. S.; Kim, H. J.; Yang, W.; Choi, J. Y., *Small* **2017,** *13* (39), 1701306.

130. Choi, S. H.; Kim, H. J.; Song, B.; Kim, Y. I.; Han, G.; Nguyen, H. T. T.; Ko, H.; Boandoh, S.; Choi, J. H.; Oh, C. S., *Adv. Mater.* **2021,** *33* (15), 2006601.

131. Zhang, Z.; Chen, P.; Duan, X.; Zang, K.; Luo, J.; Duan, X., *Science* **2017,** *357* (6353), 788-792.

132. Kim, H.; Lu, K.; Liu, Y.; Kum, H. S.; Kim, K. S.; Qiao, K.; Bae, S.-H.; Lee, S.; Ji, Y. J.; Kim, K. H., *ACS Nano* **2021,** *15* (6), 10587-10596.

133. Han, X.; Yu, J.; Li, Z.; Wang, X.; Hao, Z.; Luo, Y.; Sun, C.; Han, Y.; Xiong, B.; Wang, J., *ACS Appl. Electron. Mater.* **2022,** *4* (11), 5326-5332.

134. Sangiovanni, D. G.; Gueorguiev, G.; Kakanakova-Georgieva, A., *Phys. Chem. Chem. Phys.* **2018,** *20* (26), 17751-17761.

135. Manzo, S.; Strohbeen, P. J.; Lim, Z. H.; Saraswat, V.; Du, D.; Xu, S.; Pokharel, N.; Mawst, L. J.; Arnold, M. S.; Kawasaki, J. K., *Nat. Commun.* **2022,** *13* (1), 4014.

136. Kim, H.; Lee, S.; Shin, J.; Zhu, M.; Akl, M.; Lu, K.; Han, N. M.; Baek, Y.; Chang, C. S.; Suh, J. M., *Nat. Nanotechnol.* **2022,** *17* (10), 1054-1059.

137. Zhou, G.; Younas, R.; Sun, T.; Harden, G.; Li, Y.; Hoffman, A. J.; Hinkle, C. L., *ACS Nano* **2022,** *16* (11), 19385-19392.

138. Hasegawa, S.; Ino, S.; Yamamoto, Y.; Daimon, H., *Jpn. J. Appl. Phys.* **1985,** *24* (6A), L387. DOI 10.1143/JJAP.24.L387.

139. Trevor, F.; Weightman, P. In *Laser reflectometry for in-situ monitoring of the epitaxial growth of thin films*, Proc. SPIE, **1995**; pp 106-115.

140. Jacobsson, D.; Panciera, F.; Tersoff, J.; Reuter, M. C.; Lehmann, S.; Hofmann, S.; Dick, K. A.; Ross, F. M., *Nature* **2016,** *531* (7594), 317-322. DOI 10.1038/nature17148.

141. Diallo, T. M.; Aziziyan, M. R.; Arvinte, R.; Harmand, J.-C.; Patriarche, G.; Renard, C.; Fafard, S.; Arès, R.; Boucherif, A., *Small* **2022,** *18* (5), 2101890.

142. Chen, J.; Zhu, E.; Liu, J.; Zhang, S.; Lin, Z.; Duan, X.; Heinz, H.; Huang, Y.; De Yoreo, J. J., *Science* **2018,** *362* (6419), 1135-1139.

143. Qiang, X.; Iwamoto, Y.; Watanabe, A.; Kameyama, T.; He, X.; Kaneko, T.; Shibuta, Y.; Kato, T., *Sci. Rep.* **2021,** *11* (1), 22285.

144. Zhang, K.; Ding, C.; Pan, B.; Wu, Z.; Marga, A.; Zhang, L.; Zeng, H.; Huang, S., *Adv. Mater.* **2021,** *33* (45), 2105079.

145. Reinhold-López, K.; Braeuer, A.; Romann, B.; Popovska-Leipertz, N.; Leipertz, A., *Procedia Eng.* **2015,** *102*, 190-200.

146. Pauc, N.; Phillips, M.; Aimez, V.; Drouin, D., *Appl. Phys. Lett.* **2006,** *89* (16), 161905.

147. Li, Q.; Zhang, J.; Meng, L.; Chong, J.; Hou, X., *J. Nanomater.* **2015,** *2015* (1), 903098.

148. Lohstroh, A.; Sellin, P.; Wang, S.; Davies, A.; Parkin, J.; Martin, R.; Edwards, P., *Appl. Phys. Lett.* **2007,** *90* (10), 102111.

149. Donmez, O.; Gunes, M.; Erol, A.; Arikan, C. M.; Balkan, N.; Schaff, W. J., *Nanoscale Res. Lett.* **2012,** *7*, 490.

150. Pandey, S.; Cavalcoli, D.; Minj, A.; Fraboni, B.; Cavallini, A.; Skuridina, D.; Vogt, P.; Kneissl, M., *Acta Mater.* **2012,** *60* (6-7), 3176-3180.

151. Kaun, S. W.; Burke, P. G.; Hoi Wong, M.; Kyle, E. C.; Mishra, U. K.; Speck, J. S., *Appl. Phys. Lett.* **2012,** *101* (26), 262102.

152. Hite, J.; Gaddipati, P.; Meyer, D.; Mastro, M.; Eddy Jr, C., *Electron. Lett.* **2014,** *50* (23), 1722-1724.

153. Wang, Z.; Goodge, B.; Baek, D.; Zachman, M.; Huang, X.; Bai, X.; Brooks, C.; Paik, H.; Mei, A.; Brock, J., *Phys. Rev. Mater.* **2019,** *3* (7), 073403.

154. Kalinin, S. V.; Ziatdinov, M.; Ahmadi, M.; Ghosh, A.; Roccapriore, K.; Liu, Y.; Vasudevan, R. K., *Appl. Phys. Rev.* **2024,** *11* (1), 011314.

155. Torrisi, S. B.; Bazant, M. Z.; Cohen, A. E.; Cho, M. G.; Hummelshøj, J. S.; Hung, L.; Kamat, G.; Khajeh, A.; Kolluru, A.; Lei, X.; Ling, H.; Montoya, J. H.; Mueller, T.; Palizhati, A.; Paren, B. A.; Phan, B.; Pietryga, J.; Sandraz, E.; Schweigert, D.; Shao-Horn, Y.; Trewartha, A.; Zhu, R.; Zhuang, D.; Sun, S., *APL Mach. Learn.* **2023,** *1* (2), 020901.